FUSION TECHNOLOGY

Annual Report of the Association EURATOM/CEA 1999

Compiled by : Ph. MAGAUD

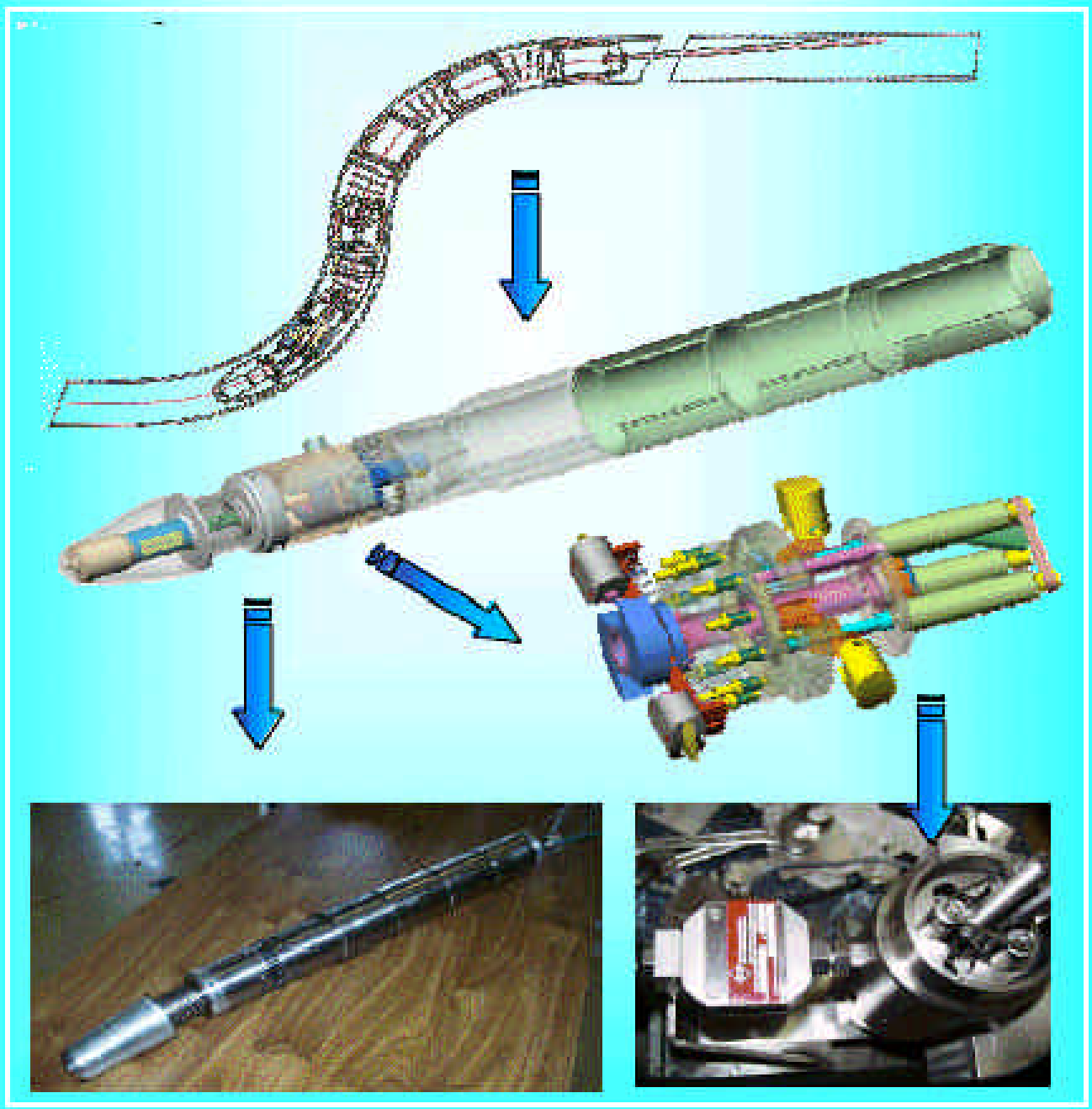

ASSOCIATION CEA/EURATOM
DSM/DRFC

CNET 96-412

Task Title : ITER OUTBOARD BAFFLE Design and analysis

INTRODUCTION

The activity concerned the final report of phase 2 of the ITER Task T232.10 (NET contract 96/412) entitled ″ITER Outboard Baffle: Design, Analysis, Technical Specification and Follow-up of Fabrication & Testing of Mock-ups & Prototypes" defined in Spring 1996 and expected initially to last until Summer 1998 (corresponding to the end of the ITER EDA). It recalls all work done by CEA on this task, in particular the last thermo-mechanical analyses, and describes the progress in manufacturing of both baffle/limiter prototypes currently ongoing at NNC (Beryllium prototype) and at Framatome/Plansee (CFC/W prototype).

1999 ACTIVITIES

In 1999, the CEA activity in the framework of phase 2 of the ITER Task T232.10 was to follow the prototype manufacturing by industry. This activity concludes the CEA contribution to this task and the report [1] presenting the status of the fabrication of the two prototypes is therefore the final report for the task.

SUMMARY OF THE THERMO-MECHANICAL ANALYSES

Thermal & thermo-mechanical analyses have been performed for the FW-panels present in the CFC-prototype and in the Be-prototype of the ITER baffle. The analyses have focused on the most-critical FW-panel designs (Be-monoblock and CFC-monoblocks) which are supposed to be tested under heat-flux conditions corresponding to the expected ITER baffle & limiter (when applicable) operating conditions. The results obtained show that all FW-panels are able to withstand the reference heat-flux when their thermo-mechanical behaviour is compared to previous small-scale mock-up testing. It must be stressed that the obtained results do not take into account fatigue phenomena, because no data are available. The only available data are those obtained with the small-scale mock-up testing. Using these data, the FW panels are expected to withstand a large number of cycles. Unfortunately, the geometry of the small-scale mock-ups were significantly different to the on used for the prototypes FW-panels. Therefore, unexpected fatigue phenomena, especially in the FW-panel corners, could occur.

CFC/W PROTOTYPE MANUFACTURING PROGRESS

The last meeting concerning the manufacturing of the CFC/W prototype was hosted by Plansee, Reutte, Austria on October 6, 1999. At this date, after an R&D phase with the goal to define the best manufacturing process, four straight CFC monoblock qualification samples were delivered by PLANSEE, two CFC monoblocks type B ("slotted monoblock") and two CFC monoblocks type C ("dovetail" monoblock). One of the type C monoblocks was sent to Forschungszentrum Jülich for high heat flux testing in the JUDITH facility and the other three mock-ups have been ultrasound tested by Framatome and will be tested in FE-200. The manufacturing of the curved monoblock was not successful at this moment.

Progress has been achieved in the manufacturing of the heat sink for the W plasma spray qualification sample (type A, flat tile) by Framatome. Three V-shaped heat sinks will be produced and delivered to Plansee. The non destructive testing procedures applied to the qualification samples and the baffle full scale prototype are available. For example, Framatome has presented the ultrasound inspections of the two type B monoblock qualification samples as well as that of the remaining type C monoblock. Plansee indicated that the comparison between the thermographic examinations carried out at Plansee and the ultrasound inspections performed by Framatome lead to quite similar results.

BERYLLIUM PROTOTYPE MANUFACTURING PROGRESS

The last meeting concerning the manufacturing of the Be prototype (at least with CEA participant), was hosted by the NET Team, Garching, Germany on September 29, 1998. At the early stage of the study, only preliminary development had been performed. The design was finalised and the material procurement was done (except for Be which was ordered). The preliminary attachment techniques were tested (HIP and EB welding). Manufacturing of the qualification samples has begun.

After this meeting, various problems were encountered in the manufacturing of the qualification samples. In particular, some failures appeared during the HIP cycle. A progress report from NNC describes these problems and the investigations performed in order to understand the reasons of the failures and to try to cure the problem. In particular, finite element calculations have been performed in support of the mechanical and chemical analyses of the failures.

Chemical interaction between the various materials (DS copper, Be and titanium) seems to be the cause of the failure. A review of recent work on bonding techniques has been performed in order to define a good solution for avoiding failures. A proposal to obtain a successful sample is expected.

CONCLUSIONS

Thermal & thermo-mechanical analyses have been performed for the FW-panels present in the CFC-prototype and the Be-prototype of the ITER baffle. Even if the used calculation models cannot predict all possible phenomena, in particular thermal fatigue, the test results will be very useful to interpret the computed results. This would allow to evaluate and interpret the results of future thermo-mechanical analyses.

CEA has followed the manufacturing of the two prototypes. In both cases, after some successful preliminary development, problems were encountered in the manufacturing of qualification samples. For the CFC/W concept, fabrication of the straight qualification samples and of the heat sink for the W plasma spray was successful, but the manufacturing of the curved monoblock presents problems. For the Be concept, some failures appear during the HIP cycle of the qualification samples and another solution has to be found.

Due to these various problems and to the time necessary to find acceptable solutions, even for the successful manufacturing of all qualification samples, the end of the manufacturing of both prototypes is not expected before the end of 2000. As a consequence, the tests under heat flux (in the FE-200 facility in Le Creusot for the CFC/W-prototype and in the Neutral Beam facilities available at JET in Culham for the Be-prototype) are not expected before spring 2001. The results of these tests will be useful to confirm the results of the calculations performed for the components.

PUBLICATIONS

[1] Compiled by L. Giancarli and J.-F. Salavy, ITER Outboard Baffle: design, analysis, technical specification and follow-up of fabrication & testing of mock-ups & prototypes.
Final report, CEA report, DRN/DMT SERMA/LCA/RT/00-2747/A, February 2000.

TASK LEADER

Luciano GIANCARLI

DRN/DMT
CEA Saclay
91191 Gif-sur-Yvette Cedex

Tél. : 33 1 69 08 21 37
Fax : 33 1 69 08 99 35

E-mail : luciano.giancarli@cea.fr

CNET 98-477

Task Title : THERMAL FATIGUE OF DIVERTOR MEDIUM SCALE COMPONENTS
200 kW electron beam gun test

INTRODUCTION

A NET contract has been launched in September 1998 (N°98.477) to cover the testing of plasma facing components in the high heat flux facility FE200 located in Le Creusot.

This test facility has been installed with European preferential support in 1990 under fusion technology task PDT2/3.

The present contract is the seventh, covering the facility operation for testing components and mock-ups for the fusion community.

The general scope of the program was to prepare and test a maximum of 5 mock-ups manufactured by different associations or contractors.

This final report covers three (3) high heat flux testing campaigns performed from january 1998(*) to November 1999.

Each test campaign has been reported (cf. [1] to [11], p7 of this report).

The total usage time of 350 h has been shared as indicated on the following list:

1. PRODIV1 - CEA 60
   "Fatigue and Critical Heat Flux testing on Prototypical Divertor mock-up PRODIV1"
   tested in January 1998.

2. PSW3 – CEA 67
   "PSW3 Screening and fatigue"
   tested in January.

3. VTMS – CEA 69
   "Vertical Target Medium Scale Mock-up"
   tested from May 1999 to November 1999.

(*) It was initially foreseen to test a wing medium scale component but this campaign was post-poned because of unavailability of the Wing due to manufacturing problems. PRODIV1 testing, already complete when the contract was signed, was designed to replace Wing testing.

1999 ACTIVITIES

CAMPAIN N° 1 : PRODIV1 - CEA 60, JANUARY 1998

A monoblock prototypical divertor mock-up was tested in FE200 during January 1998. A first screening on the mock-up showed a good global thermal behavior although some monoblock tiles were in defect. Five tiles sustained 1000 cycles at about 20MW/m² without important damage at inlet thermal-hydraulic ITER conditions (140°C, 3.5 MPa, 12m/s). However, a slight increase of surface temperature was observed after the fatigue cycling.

A final CHF testing led to a water leak at an incident maximum heat flux (IMHF) of 20.4 MW/m² for the same TH conditions with one-side uniform incident heat flux. This surprising low value of IMHF was compared with previous CEA-EURATOM data base and after analysis imputed on internal defects from manufacturing process.

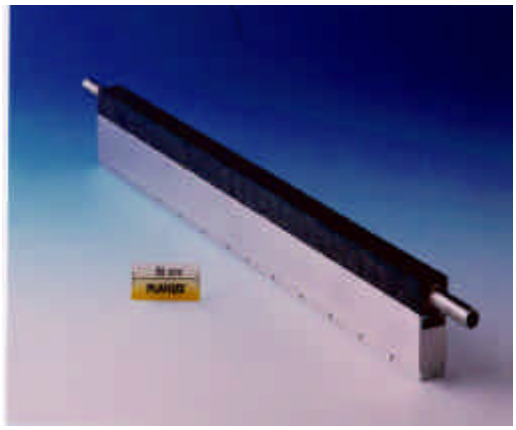

1340°C

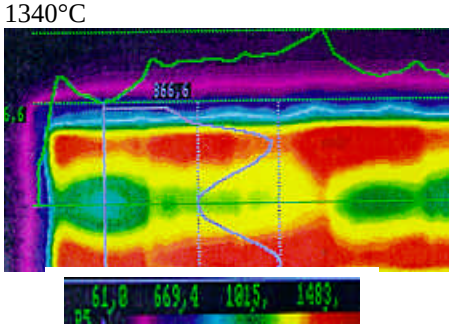

IHF = 20 MW/m², 12m/s, 3.4 MPa, 140°C

Figure 1 : Prodiv 1 mock-up & IR measurements

CAMPAIN N° 2 : PSW3 – CEA 67, JANUARY 1999

After pre-selection of samples on SATIR test bed, 4 plasma spray tungsten components were high heat flux tested on FE200 facility. Aim of the test was to rank different tungsten plasma spray deposition route.

2 components sustained incident heat flux of 3 MW/m² during 1000 cycles with surface temperature close to 600°C.

A third one showed a surface temperature as high as 800°C and the last one was clearly in defect and could not be cycled.

Finally, none of the 4 samples could survive at an incident high flux of 5 MW/m², which seems to be the limit of this technology.

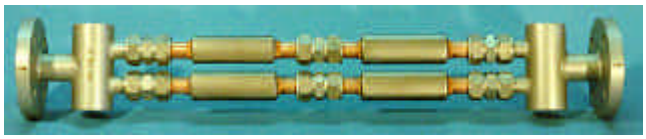

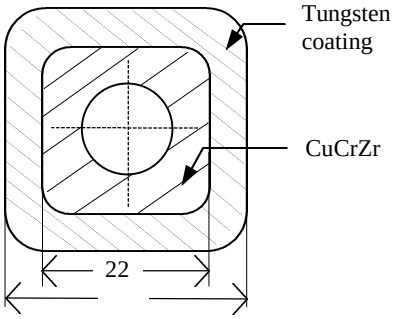

View of heated area during FE200 testing

Figure 2 : PSW3 mock-up

CAMPAIN N° 3 : VTMS – CEA 69, FROM MAY 1999 TO NOVEMBER 1999

Vertical Target Medium Scale component is a prototype of the ITER divertor vertical target, it was observed, non-destructively tested and high heat flux tested on FE200 facility Main technical points of interest are that although some internal defects from manufacturing process :

- CFC NS31monobloc part of this component sustained 2000 cycles at 18 MW/m² without failure, an increasing of power up to 30 MW/m² did not led to a critical heat flux;

- Tungsten macrobrush part sustained 1000 cycles at 10 MW/m² plus 1000 cycles at 15 MW/m² which is the maximum of power allowable for this technology. Post-testing observations showed that large teeth of Tungsten have better resistance to fatigue than small ones.

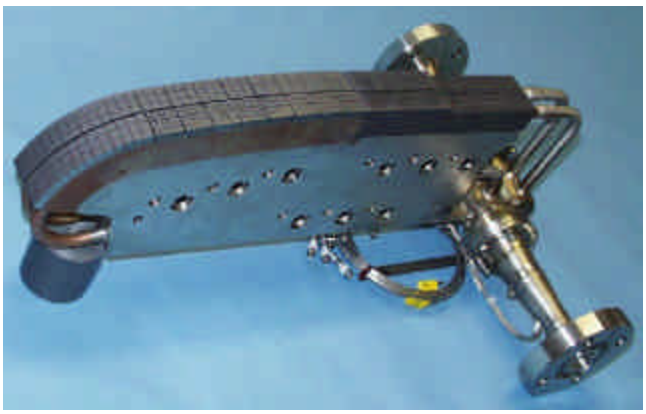

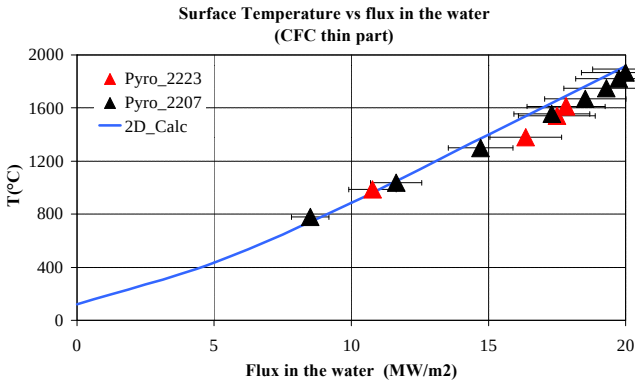

Figure 3 : VTMS Mock-up & surface temperature behavior

CONCLUSIONS

Three testing campaign in the FE200 test facility have permitted to evaluate different technologies for the plasma facing components of ITER.

Three different mock-ups have been equipped, prepared and infra-red non destructively tested in CEA prior to the heat flux testing in Framatome Le creusot. From these 3 test campaign one could deduce that :

- NB31 or NS31 macroblocs are able to sustain fatigue cycling at 20 MW/m which corresponds to ITER specifications;

- Tungsten or Wla2O3 macro-brush survive to 15 MW/m² as a maximum with strong outgassing of copper and armour erosion;

- Thick plasma spray tungsten components are able to work in fatigue cycling under an incident heat flux of 3 MW/m² (600°C on surface), they fail at 5 MW/m².

Exhaustive data and documents concerning different testing campaign are reported in the different references.

REFERENCES

[1] "Technical specifications of PRODIV1 testing on FE200"
NT/CO/99/051, P.Chappuis

[2] "Review of fatigue and critical heat flux testing on prototypical divertor mock-up PRODIV1"
NT/CO/98/003, J.Schlosser, March 1998

[3] "Fatigue and critical heat flux testing on prototypcal divertor PRODIV1 (CEA60)"
Framatome report MC/TS 97.832 B, M.Diotalevi, July 98

[4] "Technical specifications of PSW3 testing on FE200"
NT/CO/99/050, P.Chappuis

[5] "Tests SATIR sur 5 maquettes PW3 : 2669-2671-2681 et 2682"
NOTE RCQ98.007, V.Martin, Novembre 1998

[6] "Review of FE200 fatigue testing on PSW3 mock-up"
NT/CO/99/052, P.Chappuis, March 1999

[7] "PSW3 screening and fatigue testing (CEA 67)"
Framatome report MC/TS –R-99.844A, M.Febvre

[8] "Technical specifications of VTMS testing on FE200"
NT/CO/99/049, P.Chappuis

[9] "Tests SATIR sur VTMS"
NOTE PCQ/99.007, V.Martin, March 1999

[10] "Synthesis of Vertical Target Medium Scale testing"
CFP/NTT-1999.012, P.Chappuis, December 1999

[11] "Vertical Taget Medium Scale Testing (CEA 69)"
Framatome report MCTS -R-99.845A, I.Vastra

TASK LEADER

Ph. CHAPPUIS

DSM/DRFC/SIPP
CEA Cadarache
13108 St Paul Lez Durance Cedex

Tél. : 33 4 42 25 46 62
Fax : 33 4 42 25 49 90

E-mail : chappuis@drfc.cad.fr

DV4.3

Task Title : OPTIMISATION AND MANUFACTURE OF HHF COMPONENTS Study of flat tile cascade failure possibility for high heat flux components

INTRODUCTION

The object of this task was to evaluate the possibility of failure in cascade of flat tiles under convective heat flux with a glancing incidence if one tile falls off. Calculations and tests on the HHF facility FE200 are foreseen.

Preliminary works in 1999 were undertaken: definition of the geometry of heat sink for the flat tile concept and numerical analysis to study the feasibility of the tests. Finally at the end of the year a meeting was organised to define the mock-ups and the foreseen tests.

1999 ACTIVITIES

GEOMETRY OF THE HEAT SINK

The component has to be designed in order to sustain normal peak profile of 20MW/m^2. This leads to the choice of an hypervapotron for the cooling of the heat sink. Looking at the experience gained at JET in such a technology the geometry was defined as shown in Fig. 1.

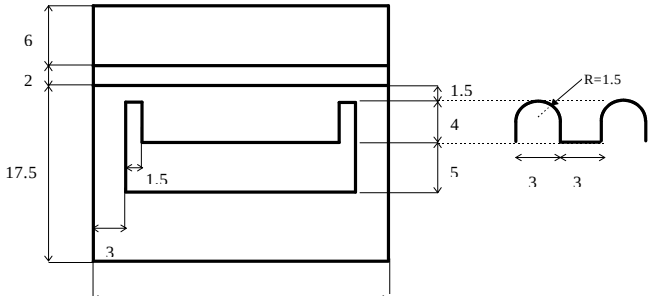

Figure 1 : Design of the hypervatron cooling tube

PRELIMINARY FINITE ELEMENT CALCULATIONS

The hypervapotron cooling tube is supposed to be covered with 6 mm thick NS31CFC flat tiles. The temperature of a tile is analysed when an adjacent tile is missing. The hypothesis for the heat flux is a 3° incident heat flux (Fig. 2).

Maximum temperature of the tiles is studied versus incident heat flux corresponding to the normal incidence. As the temperature of the CFC is very high, a special radiation law was used to take into account the impurity radiation, the carbon evaporation and the black body radiation (Fig. 3).

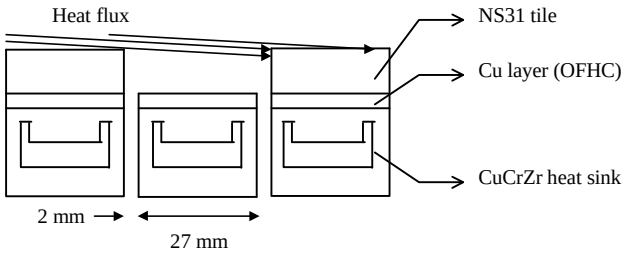

Figure 2 : Hypothesis of the calculation

This allowed to be not limited in flux during the calculation, and to be more realistic in absorbed power by the element.

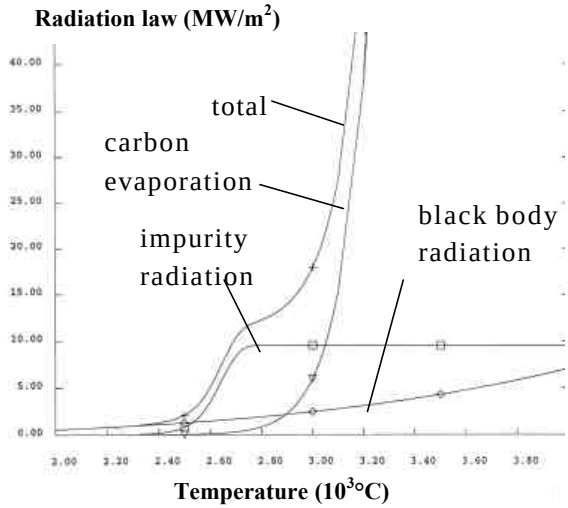

Figure 3 : Special radiation law taken into account

Four shapings of the tile were studied, the 2 first ones with respectively a radius of 1.6 and 3 mm, the 3rd and 4th ones with respectively a chamfer of 1.5 and 2 mm up to the middle of the tile and a small radius of 1.6mm. The results are presented Fig. 4 in terms of maximum tile temperature and maximum Cu layer temperature for each of the 4 geometries (Fig. 4).

Assuming a maximum temperature of 650°C at the CFC/Cu bond, the maximum acceptable heat flux would be about 5MW/m^2 for cases 1 and 2 and around 8 MW/m^2 for cases 3 and 4. The probability to have a de-bonding at 10MW/m2 is then very high. In order to simulate this loading on the high heat flux (HHF) facility FE200, the heat flux through the Cu-layer was studied; the profile of this heat flux along the 2.7cm of the width is shown Fig. 5.

On this figure the absorbed flux over the total incident heat flux is mentioned. A case-1 profile could be easily reproduced on the FE200 facility.

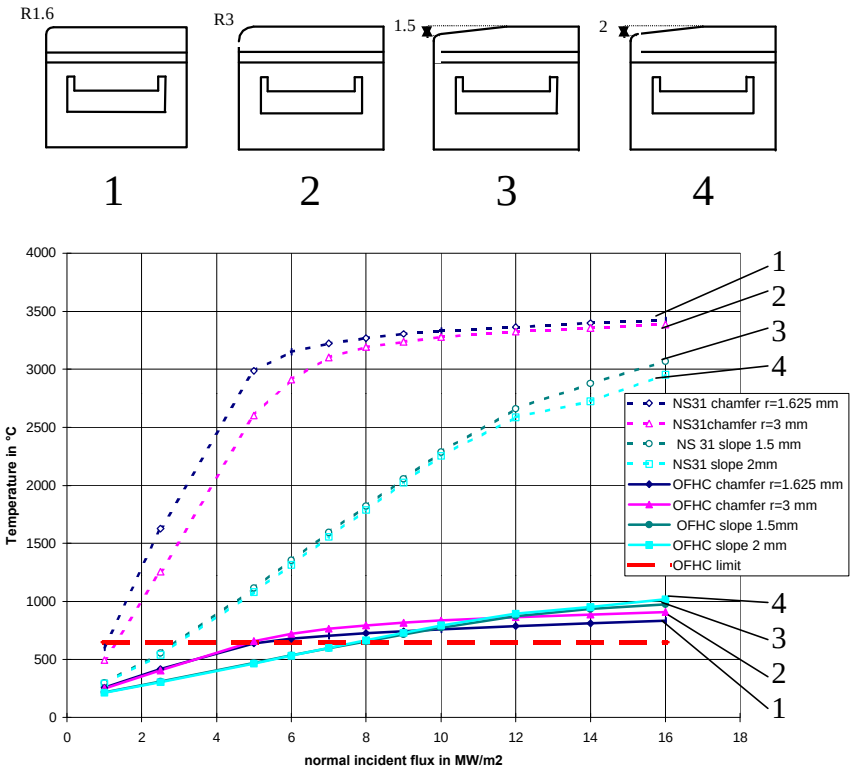

Figure 4 : Surface and Cu-layer temperatures vs. normal heat flux for various shapings

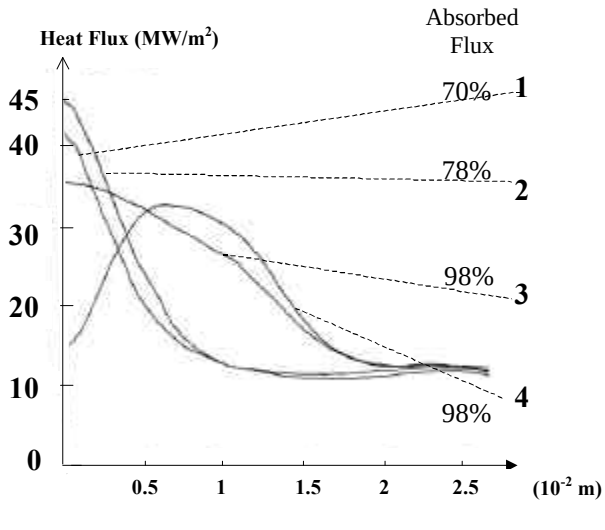

Figure 5 : Heat flux through the cu layer along the tile width

DEFINITION OF THE FUTURE TESTS

1. The following input parameters will be assumed for the experimental tests:

   - Heat flux normal to the heated surface: 10 MW/m^2
   - Angle of incidence of the heat flux: 3°
   - Coolant conditions: 100 °C, 3.5 MPa, 12 m/s

2. Two mock-ups will be manufactured with a CFC (SEP NB31) armour (tiles 20 x 27 x 6 mm) and two ones with a W armour (tiles 6 x 6 x 6 mm). The gap between each tile will be ~1 mm.

3. One mock-up with a CFC armour and one with a W armour will be used for the thermal fatigue test (1000 cycles at 20 and 15 MW/m2 for the CFC and W armour, respectively).

4. One mock-up with a CFC armour and one with a W armour will be used for the cascade failure test.

   Two CFC tiles, located 100 mm from each end of the mock-up, will have a reduced thickness (5 mm instead of 6 mm) to simulate the loss of a tile. To prevent excessive CFC sublimation, the leading edge of one of the adjacent tiles will be chamfered.

   A few W tiles, located 100 mm from each end of the mock-up, will have a reduced thickness (5 mm instead of 6 mm) to simulate the loss of a tile.

5. The study on the possible cascade failure will be performed in two ways: (a) applying a heat flux normal to the surface which simulates the computed heat flux through the pure Cu interlayer, (b) applying a heat flux with a glancing incidence of 3°.

6. The mock-ups will be instrumented with 6 thermocouples each, 3 located in the armour and 3 in the heat sink.

CONCLUSION

The results of the numerical analysis showed that soon after a flat tile is lost a CFC temperature exceeding 3000 °C is reached on the leading edge of the adjacent tile. Then this temperature goes down to ~2100 °C when CFC starts to erode. The heat flux through the pure Cu interlayer was also computed assuming different erosion depths.

The work concerning this task is now well engaged, it will be pursued with tests on the FE200 facility, these tests being now well defined.

REFERENCES

[1] Compte rendu de réunion “hypervapotron meeting” du 17 juin 1999 à JET (UK), NT/CFP//99/008, F. Escourbiac, juin 99

[2] Study of flat tile cascade failure possibility for high heat flux components. Preliminary calculations, N. Curt, J. Schlosser, Jan. 00

TASK LEADER

J. SCHLOSSER

DSM/DRFC/SIPP
CEA Cadarache
13108 St Paul Lez Durance Cedex

Tél. : 33 4 42 25 25 44
Fax : 33 4 42 25 49 90

E-mail : schlos@drfc.cad.cea.fr

DV6

Task Title : N-IRRADIATION OF REFERENCE HHF MATERIALS AND COMPONENTS
Pre and post irradiation thermal properties of high thermal conductivity CFCs

INTRODUCTION

Carbon Fiber Composites are promising material in High Heat Flux (HHF) components such as divertor, limiters or baffles. The chemical erosion and the radiation enhanced sputtering (RES) have to be suppressed to improve the CFC_s resistance to water/oxygen. It has been shown that adding small concentrations of SiC reduces the hydrocarbon formation, the chemical erosion and the total tritium retention ; and moreover increases the oxidation resistance in steam. Société Européenne de Propulsion (SEP) has developed a Si doped CFC called NS31. The neutron irradiation effects on the CFC_s thermal conductivity is a crucial problem especially at low irradiation temperature [1].

The aim of this task is to give the thermal properties of the two CFCs materials (NB31, NS31) chosen as reference HHF components CFC_s in the new design of ITER. NB31 and NS31 thermal properties will be measured before and after irradiation in HFR PETTEN at low irradiation temperature (200°C) and at two damage levels : 0.2 and 1 dpa.g.

1999 ACTIVITIES

PRE IRRADIATION THERMAL PROPERTIES [2]

NB31 is a 3D CFC constituted by a NOVOLTEX preform, with P55 ex-pitch fibers in x direction and ex-PAN fibers in y direction. This preform undergoes a needling which gives an orientation in z direction. The densification is made by chemical infiltration of pyrocarbon followed by a graphitization treatment. A last phase of densification is operated by chemical infiltration of pyrocarbon followed by a pitch impregnation. The NB31 density is about 1.95 g/cm^3.

NS31 is a N31 CFC but the last phase of densification by chemical infiltration of pyrocarbon is followed by an injection of liquid silicon leading partly to the formation of SiC. NS31 density is about 2.1 g/cm^3, its porosity is 3 - 5% and it contains about 8 - 10% at of Si.

The thermal diffusivities of these 2 CFC_s measured by Laser Flash Method are given in the following table :

Temperature (°C)	Thermal diffusivity in mm^2/s					
	NB31			NS31		
	x dir.	y dir.	z dir.	x dir.	y dir.	z dir.
25	248	78	81	214	105	85
400	82	26	27	73	34	28
800	46	15	16	42	20	15

The heat capacities of these CFC_s are given in the following table :

Temperature (°C)	Heat capacity ($J.kg^{-1}.K^{-1}$)	
	NS31	NB31
25	710	723
100	898	918
200	1 128	1 173
300	1 285	1 352
400	1 390	1 473
500	1 461	1 556
600	1 511	1 615
700	1 546	1 657
800	1 572	1 688

The evolution of CFC_s thermal conductivity (K) is performed using the equation $K = D.\rho.Cp$ where D is the thermal diffusivity, ρ the density and Cp the heat capacity. The results are given in the following table :

Temperature (°C)	Thermal conductivity in $W.m^{-1}.K^{-1}$					
	NB31			NS31		
	x dir.	y dir.	z dir.	x dir.	y dir.	z dir.
25	352	110	114	330	159	130
400	238	75	79	220	101	83
800	154	51	53	144	66	52

NB31 and NS31 thermal conductivities in the high conductivity direction at 800°C are 154 $W.m^{-1}.K^{-1}$ and 144 $W.m^{-1}.K^{-1}$ respectively. These values are a little lower than required value (175 $W.m^{-1}.K^{-1}$).

In x direction NB31 and NS31 thermal conductivities are similar ; in the y and z directions NS31 measured values are higher than those of NB31 which is a silicon free CFC. This is surprising ; the adding of silicon in the CFC would normally lead to a decrease of the thermal conductivity.

REPORTS AND PUBLICATIONS

[1] Neutron irradiation effects on carbon based materials at 350°C and 800°C
JP. BONAL, C.H. WU
J. Nucl. Mater. 277 (2000) p. 351-359

[2] Thermal properties of carbon Fiber Composites before irradiation in PARIDE 3/4 experiment
JP. BONAL
DMT/SEMI/LM2E/RT2004

TASK LEADER

JP. BONAL

DRN/DMT/SEMI/LEMA
CEA Saclay
91191 Gif-sur-Yvette Cedex

Tél. : 33 1 69 08 50 58
Fax : 33 1 69 08 90 82

T222.4 ter A

Task Title : MANUFACTURE AND TESTING OF PERMANENT COMPONENTS OPTIMISATION OF COOLING SYSTEM Critical heat flux and thermo-hydr. of representative elements, non destructive testing, calibrated defects, heat load influence (first part)

INTRODUCTION

The object of this task was a comparison of CHF obtained in various test facilities on Glidcop castellated tubes and the characterisation of the limits of prototypical vertical target CFC mock-ups.

The round robin tests confirmed the good results obtained at CEA on Glidcop castellated tubes whereas lower CHF values were obtained on the prototypical CFC mock-ups. This reduction was attributed to defects from the manufacturing process.

The work has been completed in 1999 and the final report achieved [1]. We summarise here the main results.

Figure 1 : ST22bis in EB1200

Figure 2 : ST22ter in PBEF

1999 ACTIVITIES

ROUND ROBIN TESTS

Tests were performed on the EB1200 at Sandia Nat. Lab. Albuquerque (Fig.1) and on the PBEF (Particle Beam Engineering Facility) of JAERI (Fig. 2) respectively in Oct. 97 and in Oct. 98.

At SNLA the same thermal hydraulics conditions, as in CEA, were used (P≈3.5MPa, Tin = 135°C), whereas the tests at JAERI were done at room temperature, varying the pressure drop to obtain the good subcooling.

At Jaeri the gaussian incident profile was roughly a double of the reference one.

PROTOTYPICAL MOCK-UPS

Two tube-in-tile CFC mock-ups were tested on the FE200 facility in Le Creusot : PRODIV1 and PRODIV2. These mock-ups were manufacture by Plansee and were unfortunately not defect free as shown by SATIR and FE200 testings (Fig 3).

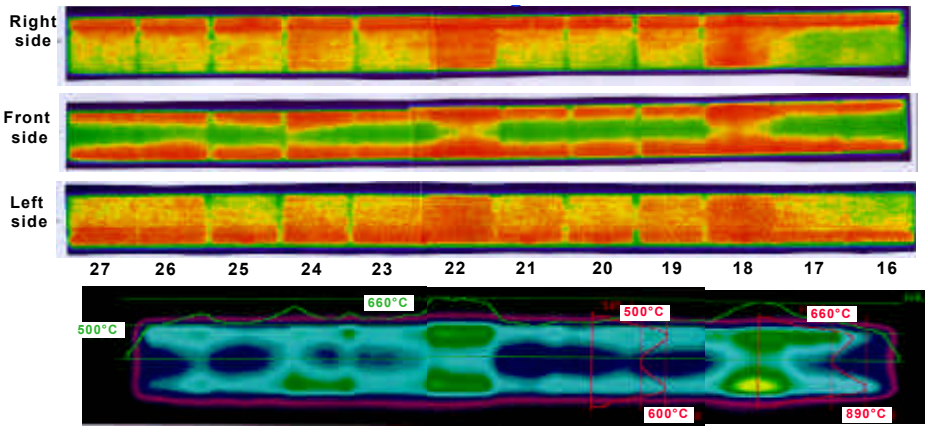

Figure 3 : SATIR tests and FE200 screening at 11 MW/m^2 showing defects on PRODIV2

PRODIV1 was extensively tested (Jan. 1998) both under fatigue cycling (1000 cycles at 20 MW/m^2) and at CHF with flat heat-flux profile (Fig.4). PRODIV2 was only tested at CHF with a 200mm reference peaked heat-flux profile (Fig.5).

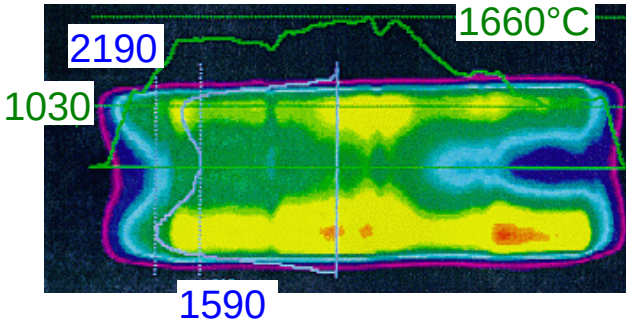

Figure 4 : PRODIV1 under 100 mm uniform heat flux just before CHF, Shot 2049, 47 kW, 20MW/m²

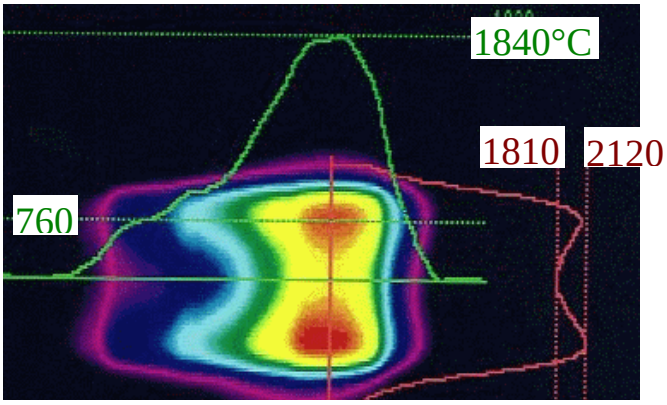

Figure 5 : PRODIV2 under 200 mm peaked heat flux just before CHF, Shot 2094, 45 kW, 29 MW/m^2

CRITICAL HEAT FLUX RESULTS

The round robin tests confirmed well the results obtained at CEA in previous studies. Unfortunately, if PRODIV1 sustained well the 1000 cycles at 20 MW/m^2, the CHF results on the prototype mock-ups were reduced of about 20%. These bad results were attributed to defects in the bonds between CFC and copper or between copper and Glidcop leading to a concentration of the heat flux.

Table 1 : Interpolated CHF results ($DT_{sub,out}$=100°C, V=12m/s)

Mock-up		ICHF (MW/m^2)		Pressure drop (MPa/m)	Pumping power (W/m)
		flat	peaked		
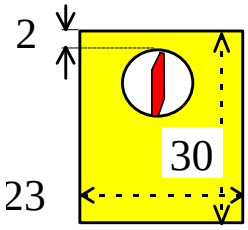	CEA ST22	27-30	30-37	0.61	428
	SNL ST22bis	27.4	33		
	JAERI ST22ter		35-37		
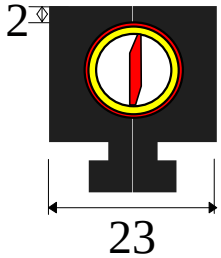	CEA Prodiv1	~22		0.61	428
	CEA Prodiv2		~30	0.61	428

POST-TEST EXAMINATION

After tests PRODIV1 and PROVID2 were cut for metallographic examination near the CHF location. For PRODIV1 the CHF occurred at the contact point of the swirl tape with the top of the tube (Fig.6, 7 and 8) but it was not the case for PRODIV2 (Fig.9)

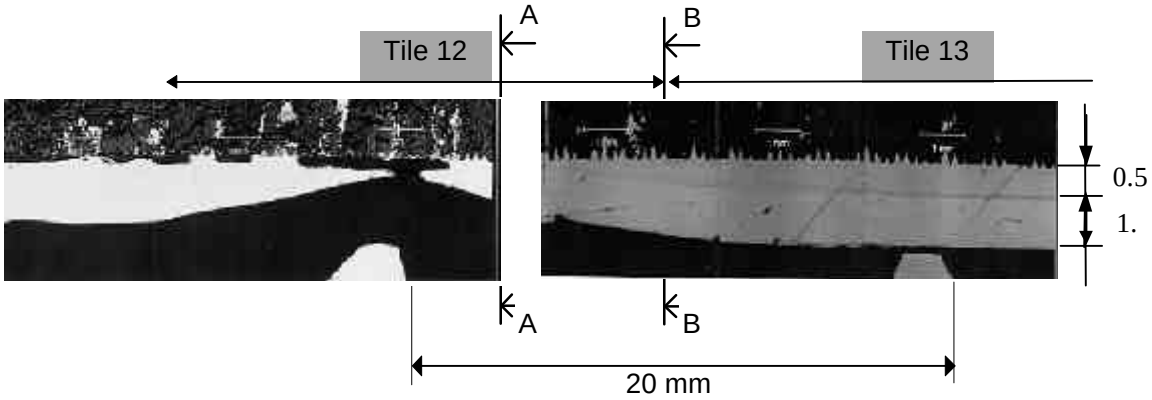

Figure 6 : Metallographic examination of PRODIV1 after CHF under uniform incident heat flux (22MW/m^2, 140°C, 12m/s, 3.5 MPa)

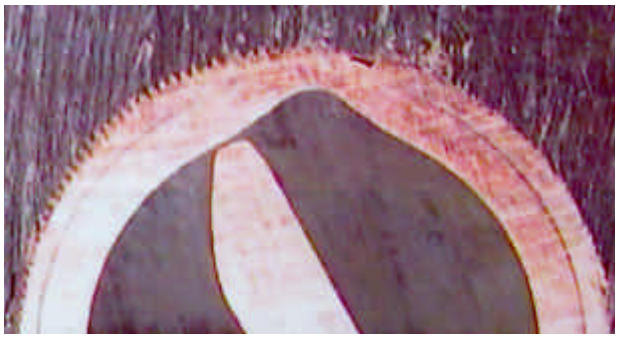

Figure 7 : Destructive examination of tile 12 after CHF, cross section AA near the middle of the tile

Figure 8 : Destructive examination of tile 12 after CHF, cross section BB on the side of tile 12

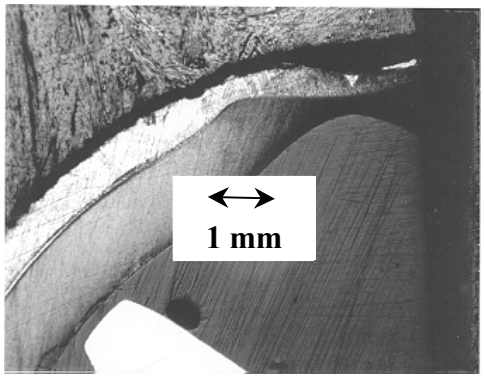

Tile 21

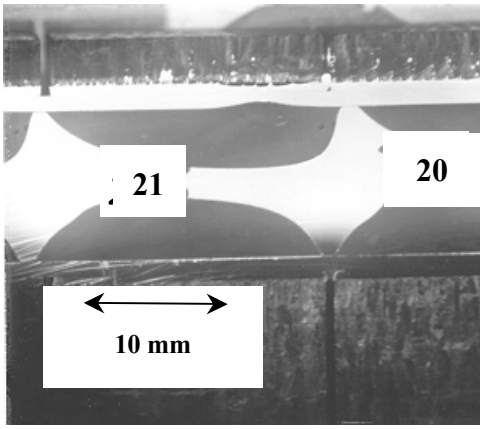

Figure 9 : Metallographic examination of PRODIV2 after CHF under peaked incident heat flux (30MW/m^2, 140°C, 12m/s, 3.5 MPa)

MISCALLENOUS

In order to improve the thermal hydraulic behaviour of the swirl tubes it was decided to try to braze the swirl tape against the internal wall (no gap between tape and wall, better exchange due to a fin effect). Several attempts were done with a brazing foil stuck on the side of the tape. Poor results were obtained, the main difficulty being the tolerances on the swirled tape diameter. A process was imagined which consists on the swirling of a wider tape already equipped with the brazing material, the swirled tape being then machined with a tolerance H8F8 (0.07mm). This was, unfortunately, not pursued.

The study about subcooled boiling heat transfer correlation in swirl tubes was completely reviewed in regards to the results obtained in T222.4bis (previous task). The work was done in the frame of a engineering degree thesis for Politecnico di Torino. The thesis presents an original error analysis and conclude to the good agreement with the CEA correlation developed in 91-95.

CONCLUSION

Important work was done in the frame of this task demonstrating that the monoblock tile concept was able to sustain 20MW/m^2 with a CHF for a peaked profile in the order of 30 MW/m^2 [2][3]. With regards to important defects found in the mock-ups at the different bonds an improvement of the fabrication has to be researched.

REFERENCES

[1] *Final report, Task T222.4ter,* J.Schlosser, , CFP/NTT-1999.001, Dec. 99, J.Schlosser.

[2] Critical Heat Flux Analysis and R&D for the Design of the ITER Divertor, A. R.Raffray, J.Schlosser, M.Akiba, M. Araki, S.Chiocchio, D.Driemeyer, F.Escourbiac, S.Grigoriev, M.Merola, R.Tivey, G.Vieider, D.Youchison, *Fusion Engineering & Design 45 (1999) 377-407.*

[3] Round Robin CHF Testing of ITER Vertical Target Swirl Tube. D.L. Youchison, J. Schlosser, F. Escourbiac, K. Ezato, C.B. Baxi, 18th SOFE, Albuquerque, Oct.99.

TASK LEADER

J. SCHLOSSER

DSM/DRFC/SIPP
CEA Cadarache
13108 St Paul Lez Durance Cedex

Tél. : 33 4 42 25 25 44
Fax : 33 4 42 25 49 90

E-mail : schlos@drfc.cad.cea.fr

T222.4 ter B

Task Title : MANUFACTURE AND TESTING OF PERMANENT COMPONENTS OPTIMISATION OF COOLING SYSTEM Critical heat flux and thermo-hydr. of representative elements, non destructive testing, calibrated defects, heat load influence (second part)

INTRODUCTION

The object of this task was to evaluate the possible detection of defects on the infrared test bed SATIR and their propagation under fatigue testing.

In 1999 a vertical target medium scale component, prototype of ITER divertor was fabricated with calibrated defects and extensively tested.

The mock-up was made of 2 parts : a part in CFC (monoblocks) and a part in Tungsten (teeth). The both parts were manufactured with artificial defects.

All the tests concerning this task were achieved, the remaining work being to perform finite element calculations for correlation with defect detection and propagation.

1999 ACTIVITIES

DESCRIPTION OF THE MOCK-UP

A view of the mock-up is given Fig.1: tiles 1 to 11 are CFC monoblock, tiles 12 to 19 are W macrobrush. For monoblocks the internal Glidcop tube is Ti brazed to the copper cylindrical layer of the CFC (carbon fibre composite), this layer is obtained by the AMC (active metal casting) process. For the W macrobrush tiles, the flat copper layer is EB (electron beam) welded to the CuCrZr heat sink.

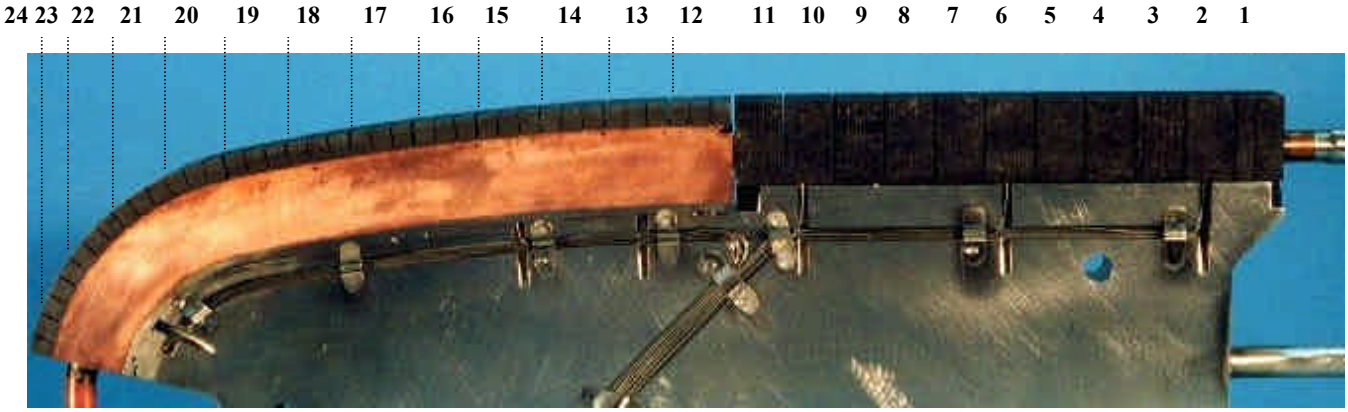

Figure 1 : VTMSdef Mock-up (11 monoblock CFC tiles and 13 macrobrush W tiles)

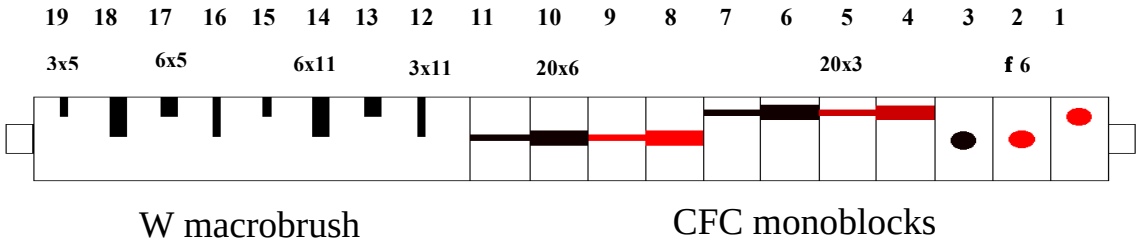

Figure 2 : Defect geometry (in mm) and location
(in red for monoblock defect at the bond between AMC and glidcop tube)

SATIR TESTING

The mock-up was tested on SATIR (Station d'Acquisition et de Traitement Infrarouge) test bed before and after fatigue test. A transient of the tile surface temperature is observed during a hot cold water shock. The appearance of defects are easier on the CFC part (Fig.3).

On the CFC part the defected tiles were classified as D1 and D2 :

D1 : if 3 < DTref (°C°) < 6 and DTzone > 4 : small defect;
D2 : if DTref(°C) > 6 : larger defect.

Dtref is the maximum range of the transient temperature difference between the considered tile zone and a reference corresponding tile zone chosen as a good one.

Dtzone is the maximum range of the transient temperature difference between the maximum temperature and the minimum temperature of the considered tile zone.

Each tile is divided in 3 zones : 2 lateral ones and a central one, theoretically colder because of better cooling.

- This classification (Table 1) gives results slightly different from IR picture analysis (Fig. 3). For example, tile 11 appears clearly hotter on picture but defect is not detected by the classification.
- Comparison with defect locations show that defects of brazing are well detected (4/5) although defects on AMC not (2/6).
- Lateral defects are more detectable than central ones : 3/4 vs. ¼ in case of longitudinal shapes.
- Central defects are more detectable than lateral ones in case of circular shapes : 2/2 vs. 0/1.

FATIGUE TESTS

The tests on the EB facility of "Le Creusot" (FE200) were performed in 5 steps :

- Step 1 : Initial screening at 12 MW/m² of the whole mock-up;
- Step 2 : Cycling on CFC (2 zones) ~12 MW/m² and W (2 zones) ~10 MW/m² at (500 cycles);
- Step 3 : Intermediate screening at 12 MW/m² of the whole mock-up;
- Step 4 : Cycling on CFC (2 zones) at 12 MW/m² and W (2 zones) at 15 MW/m² (500 cycles);
- Step 5 : Final screening at 12 MW/m² of the whole mock-up.

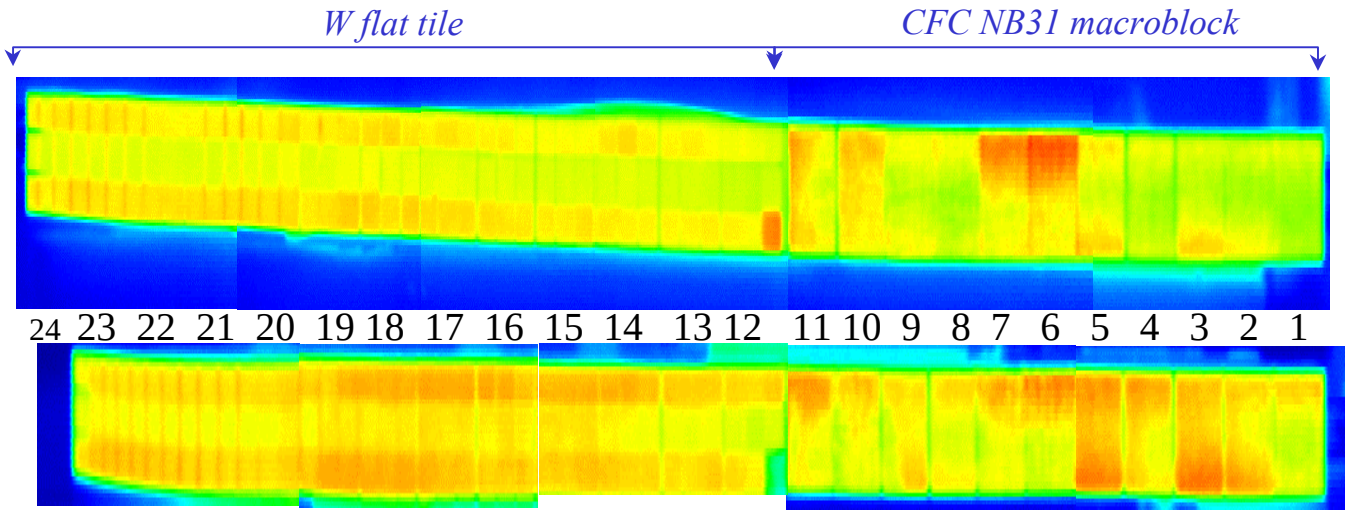

Figure 3 : SATIR view of VTMSdef before/after fatigue testing

Table 1 : Defect classification on zones of the CFC monoblocks
(above : before fatigue tests, below: after fatigue tests)

Tile 11	Tile 10	Tile 9	Tile 8	Tile 7	Tile 6	Tile 5	Tile 4	Tile 3	Tile 2	Tile 1
				D2	D2					
	D2			D2	D2	D1		D1	D1	
								D1	D1	

Tile 11	Tile 10	Tile 9	Tile 8	Tile 7	Tile 6	Tile 5	Tile 4	Tile 3	Tile 2	Tile 1
D1	D1			D2	D2	D1	D1			D1
	D1			D2	D2	D2		D1	D1	
		D1						D1	D1	

FE200 screening detected systematically brazing defects : tiles 3; 6; 7; 10 and 11, tube braze defect are not so clearly visible (tiles 2; 4; 5; 8 an 9 are the most healthy).

This indicates that defects location should be checked by destructive analysis after at the end of the study.

Initial and intermediate screening of W straight part are available at 10 MW/m², however IR pictures are hardlyy analysable, moreover, fatigue cycling led to homogenisation of surface temperature.

It was observed at reception of the mock-up that a macrobrush tooth was in defect due to e-beam welding problem : this tile fell after (500 cycles at 10 MW/m² + 400 cycles at 15 MW/m²). One can note that although a very bad thermal contact of this tooth, it does not appear clearly on FE200 infra red pictures but does appear on SATIR pictures.

Globally, we did not observe a strong propagation of defects : infra-red image was hotter after fatigue cycling, both on CFC and W but hot spots did not really developed. In case of CFC part, finite element calculations would help us to determine evolutions of the defect dimensions.

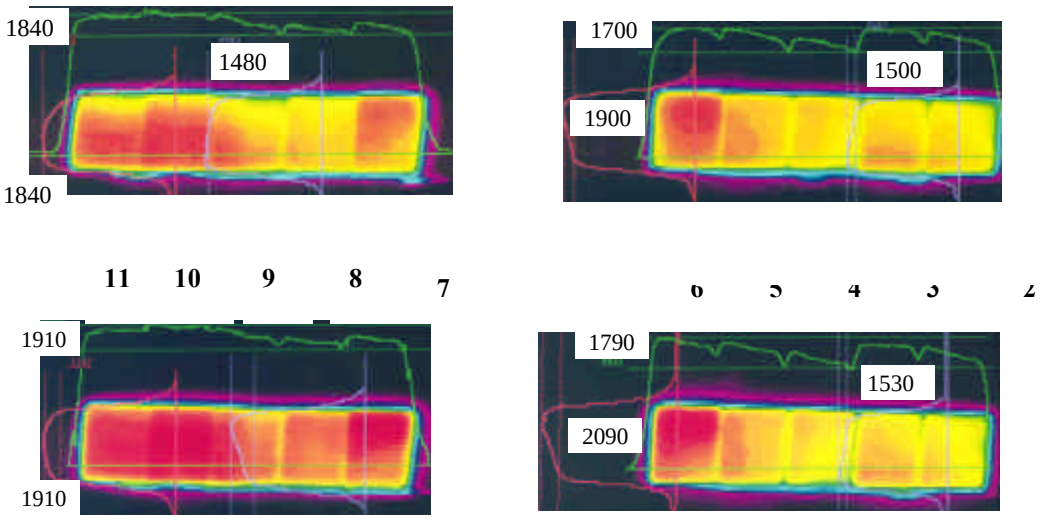

Figure 4 : Intermediate and final screening on CFC part
(above : shot 2243 11.4MW/m², below : shot 2257 11MW/m²)

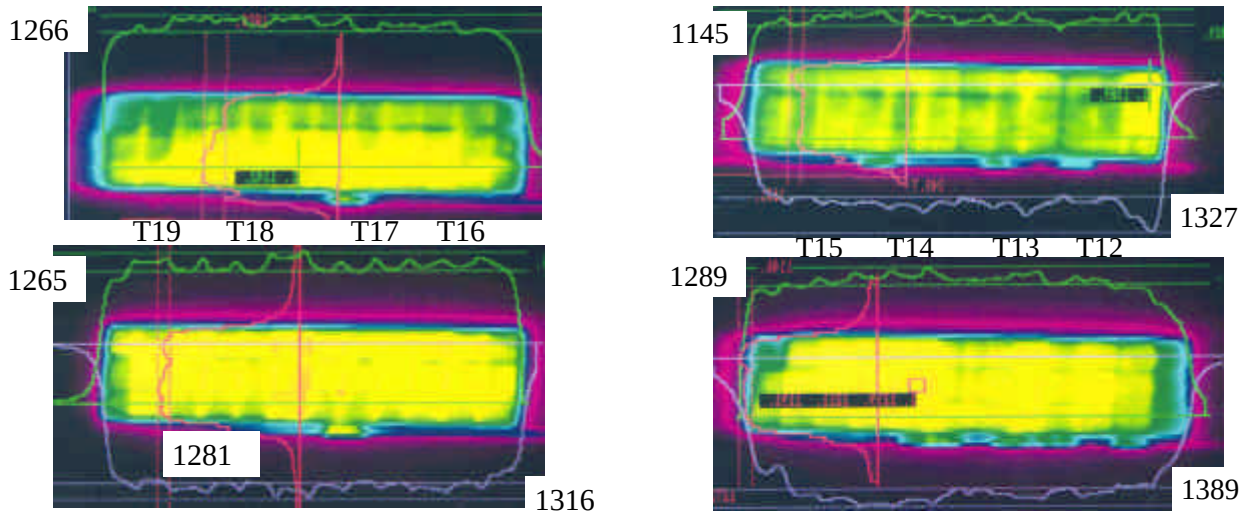

Figure 5 : Intermediate and final screening on W part
(above : shot 2244 10 MW/m², below : shot 2258 10.5MW/m²)

CONCLUSION

Vertical Target Medium Scale component « VTMSdef », prototype of the ITER divertor vertical target with calibrated defects at the inner interfaces was SATIR and FE200 tested.

Main results of the campaign testing are :

- calibrated defects propagated slowly both in CFC and W areas after 1000 cycles at ~10MW/m² (last 500th at 15 MW/m² on W).;
- SATIR and FE200 are well correlated on monoblock part of the mock-up. SATIR points out essentially a propagation of AMC defects;
- W part is not easily observable both on FE200 and SATIR facilities and comparison is difficult.

Next step of the study would be based on 3D finite element calculations correlated to experimental defects detection and propagation.

REFERENCES

[1] “Review of vertical target medium scale VTMSdef testing”, J. Schlosser, to be published.

[2] Tests SATIR sur VTMSdef avant FE200, NT/PCQ/99/0031 - V.Paulus, 03/99.

[3] Demande d’essais FE200, Maquette VTMSdef, DRFC/SIPP/99/172 - P.Chappuis, 07/99.

[4] Maquette VTMSdef - Offre F01287, M. Febvre, 09/99.

[5] “Vertical Target Medium Scale mock-up with defects VTMSdef – CEA70 ”, Framatome report, I.Vastra, to be published.

[6] “Definition and location of calibrated defects for monoblock type mock-ups”, J.Schlosser, IR IV-1 of Task T222.4ter (Subtask T222.15), NT/CO/98/16 – 08/98.

[7] Tests SATIR sur VTMSdef après FE200, NT/PCQ/00/XXX, to be published - V.Paulus, 02/00.

TASK LEADER

J. SCHLOSSER

DSM/DRFC/SIPP
CEA Cadarache
13108 St Paul Lez Durance Cedex

Tél. : 33 4 42 25 25 44
Fax. : 33 4 42 25 49 90

E-mail : schlos@drfc.cad.cea.fr

PPA 1.1.1

Task Title : HHF PLASMA-FACING MATERIALS INTERACTION PLASMA/ARMOR MATERIAL AND LIFETIME

INTRODUCTION

The objective of this task is to identify potential candidate materials to be used as armor in HHF components of a Fusion Power Plant (FPP). Up to now, the development of armor materials has been performed only for present-day machines (e.g., JET, Tore Supra, Asdex) and for next-step machines such as NET and ITER. Although the surface heat fluxes in these machines are similar or even higher than that expected for HHF-FPP, the expected operating conditions in a FPP are much more severe due to the high energy envisaged for plasma particles (links with charge-exchange process) and, even more important, to the very high neutron flux for which no experimental data are available.

1999 ACTIVITIES

IDEAL QUALITATIVE CHARACTERISTICS OF A FPP PF MATERIALS FOR HHFC

An ideal HHFC-PFM should present the following, characteristics:

1) capability to withstand high surface heat fluxes, which means a) good thermo-mechanical properties at high temperature, b) high-thermal conductivity, c) sublimation prior to melting in order to avoid surface deformation, chemical stability at high temperature;

2) limited impact of neutron irradiation, which means to maintain acceptable thermo-mechanical properties (including low DBTT) after submission to a FPP divertor-relevant neutron fluence (some MWa/m^2) and to show low swelling;

3) attractive safety features such as a) low Tritium inventory (including co-deposition), b) low afterheat, c) low production of long-term radioisotopes;

4) good compatibility with plasma, which means: a) low erosion rate (e.g., physical and chemical sputtering, charge-exchange sputtering), b) low Z (especially for significant erosion and for FW);

5) easy fabrication which means acceptable workability at room temperature and easy joining and compatibility with appropriate substrates.

No material is simultaneously the best option for each of the item in the list. Moreover, the improvement of one characteristics is sometime at the expenses of another one. Therefore, a reasonable compromise, which depends also on the assumed FPP specifications, is required.

LEARNING ON HHF PF MATERIALS FROM ITER R&D ACTIVITY

ITER is undoubtedly the project which looked in more deeply into the field of HHF plasma-facing materials. Several analyses and experimental campaigns have been performed for the ITER-FDR armor material candidates, including low-fluence neutron irradiation. Three materials were initially retained for use as plasma-facing materials: Beryllium, Carbon-Fiber Composites (CFC) and Tungsten alloys [1, 2].

Their potential lifetime as armor material for ITER-FDR divertor was estimated. After such an evaluation only CFC and W-alloy were retained mainly because of their better resistance to high temperatures and to thermal shocks.

Among this two materials, low-fluence neutron irradiation experiments and Tritium inventory evaluation (in particular, T-codeposition) indicated that only W-alloys has the potential for use in FPP operating conditions, despite some identified shortcomings such as the high irradiation-induced DBTT and the high induced radioactivity both in short term (afterheat) and in the long term (waste).

In principle, an appropriate choice of the alloying elements and of the fabrication procedure (e.g., grain size) could lead to an improvement of such characteristics. Examples of presently considered alloys are, for instance, W-Re, W-La_2O_3, W-Mo-Y-Ti, and plasma-sprayed W with various proportions of the different elements. However, up to now, these potential improvement (more relevant for a FPP than for ITER) have been only little investigated [3, 4].

In the framework of the ITER R&D program on HHF armor materials, the EU-HT was charged to irradiate various grades of the candidate materials, the irradiation being held in HFR and the post-irradiation examinations and tests performed at FZJ.

Unfortunately, the irradiation of W-alloys samples were included only in PARIDE-3 and –4 which started in spring and in autumn 1999 with preliminary results expected by the end of the year 2000.

TRITIUM-RELATED CHARACTERISTICS OF CANDIDATE MATERIALS

An assessment of available data has been performed. Data have been found for most pure metals, and for C and SiC materials although fabrication methods and grades are often not clearly stated.

From the point of view of Tritium permeation and inventory, W is the most suitable metal and V and Ta are the less favorable. The trapped inventory is relatively high for Be, C, and SiC. The permeation through SiC and C is strongly dependent on porosity. More precise information about the sticking factor and neutron irradiation effects is however needed.

EXPECTED WORKING CONDITIONS IN A POWER REACTOR

In ITER-FDR the choice of armor materials have been primarily dictated by the high surface-heat flux expected in both normal and transient conditions. The expected average surface heat flux on the vertical target in the basic pulse is 5 MW/m^2, but peak heat flux of 20 MW/m^2 for 10 s ("attached" regime) are expected in at least 100 pulses. Moreover, about 3000 full-power discharge with 10 MW/m^2 are planned.

For a FPP, one can expect that the plasma behavior, both in the main plasma and in the divertor region, will be completely understood, and therefore will be well optimized and controlled. An average surface heat flux on the divertor target <5 MW/m^2 appears to be achievable through the choice of an appropriate divertor regime (e.g., "detached regime"). In this situation, W-alloy is the most reasonable choice.

Moreover, appropriate processes able to improve the radiation in the divertor region could permit to spread over larger surfaces the heat and therefore further decrease the average surface heat flux to about 2-3 MW/m^2. These values would allow to use other materials which could be preferable to W-alloys for other reasons such as irradiation resistance and activation. Medium-Z materials, including most of structural materials, could become acceptable candidates.

EXPECTED EROSION RATE FOR TUNGSTEN

Considering EU FPP plasma parameters and a limited extrapolations on the plasma physics, a preliminary estimation of the divertor armor erosion in case of use of W could be performed.

A commercial reactor could run with a steady state power removal similar to the gas box model developed by Rebut. The plasma flux would fully interact in the divertor by charge exchange maintaining a cold detached plasma.

Under these conditions, the convected particles energy to the divertor wall would be much lower than the W sputtering threshold (~150 eV), inducing a negligible wall erosion due to sputtering. This plasma behavior assumes also the suppression of phonemes as large ELMs in normal operation.

However, erosion due to high energy neutrals produced by charge exchange (CX) in the plasma core is unavoidable [5]. It concerns all plasma-facing materials including FW.

The energy of such neutrals is higher (up to 10 keV) than the W-threshold, therefore there is no significant advantage in using this material. Assuming that neutrals are generated within the plasma core and using appropriate values of maximum CX neutral flux and temperature, the W erosion by such neutrals (without taking into account re-deposition aspects) is estimated (Bodhansky formula) to be of about 2 mm/y range.

MAIN OPEN ISSUES AND REQUIRED R&D

Present uncertainties concern two main categories:

a) reactor plasma parameters: the extrapolation to reactor condition for the divertor region presents many uncertainties such as the achievable levels of surface heat flux, particle flux and their energy, impact of plasma impurities. These data strongly depend on the achievable/suitable main plasma and divertor plasma regime and on availability of plasma control techniques which cannot be fully defined today. A major uncertainty is the evaluation of neutrals flux due to CX process which may have an impact on the FW protection. The possibility of using other materials than W-alloy is strictly related to this category of uncertainties.

b) Material data, including behavior under irradiation: acceptable divertor operating conditions depends on the material properties and their stability under irradiation. Issues such as thermal conductivity reduction and embrittlement due to neutron irradiation have to be addressed with an appropriate R&D.

CONCLUSIONS

At present, W-alloys appear as the most promising armor material for FPP divertor although their characteristics in terms of neutron irradiation damages and of activation are not fully satisfactory. Moreover, CX-induced erosion, which is inevitable also for W, could lead to the requirement of a relatively low-Z armor material.

It is therefore recommended to perform a detailed assessment on the operating parameters to be assumed in the divertor region of a FPP in order to evaluate the possibility of using medium-Z materials such as steel, Ti-alloys and SiC/SiC.

REFERENCES

[1] V. Barabash, G. Vieider, et al., Plasma facing materials for ITER, ICFRM-7 (1995), Journal of Nuclear Material 233-237 (1996) 718.

[2] G. Janeschitz, et al., Divertor development for ITER, Fusion Engineering & Design 39-40 (1988) 173-187.

[3] J.W. Davis, et al., Assessment of tungsten for use in the ITER plasma facing components, Journal of Nuclear Material 258-263 (1998) 308-312.

[4] N. Yoshida, Review of recent works in development and evaluation of high-Z plasma facing materials, Journal of Nuclear Material 266-269 (1999) 197-206.

[5] N. Yoshida, Y. Hirooka, Impacts of charge-exchange neutrals on degradation of plasma-facing materials, Journal of Nuclear Material 258-263 (1998) 173-182.

TASK LEADER

Luciano Giancarli

DRN/DMT
CEA Saclay
91191 Gif-sur-Yvette Cedex

Tél. : 33 1 69 08 21 37
Fax : 33 1 69 08 99 35

E-mail : luciano.giancarli@cea.fr

PPA 1.2.1

Task Title : HIGH HEAT FLUX COMPONENTS
Water-cooled high heat flux components

INTRODUCTION

Water is the selected coolant for High Heat Flux Components (HHFC) of present-day tokamaks and for next-step devices such as NET & ITER. Therefore, a considerable experience exists in using water-coolant in fusion environment, although, even in the case of ITER, the water is at low-temperature, and low-pressure (150°C/200°C, 4 MPa).

In case of power reactor, in order to maximize the power plant efficiency, it would be desirable to use the power deposited in the divertor region for electric power production in addition to the thermal power extracted from the blanket.

The best option is to use similar coolant parameters as for the WCLL blanket which means a water-pressure of 15.5 MPa and coolant outlet temperature above 300°C. An advantage of the water-coolant is that, being water a good neutron moderator, the same coolant could be used for all PP nuclear components, i.e., divertor, blanket, shielding, and vacuum vessel.

The present work has the objective to establish the maximum surface heat flux that could be allowed in water-cooled HHFC and in particular in the divertor target.

1999 ACTIVITIES

The assessment aimed to evaluate the maximum allowable peak heat flux. It has been assumed that an uniform surface heat flux is deposited on a length of 50 cm of the divertor armor. A fixed volume heat flux per material corresponding to a neutron wall loading of 1.2 MW/m^2 was also included.

RATIONALE OF THE MATERIALS PROPOSAL

Taking into account results from a ENEA comparative study between potential candidate metallic structural materials from a thermo-mechanical point of view together with the suggestions coming from task PPA1.1 it appeared that W-alloys was the best choice as armor material, while the same W-alloy, Mo-alloys (e.g., TZM) and martensitic steel were the best performing structural materials. However, material toughness and behavior under irradiation are not so favorable for both W-alloys and Mo-alloys (severe embrittlement behavior under neutron irradiation at temperature < 500°C).

Even assuming future improvement of the material characteristics by a substantial R&D aiming to modifying both the manufacturing routes and the alloy composition, it is unlikely that low-temperature material embrittlement can be avoided.

The limited amount of experimental results presently available give the sensitivity of the W-embrittlement to the irradiation temperature; in particular it has been shown that at a neutron fluence of 5 dpa the W DBTT increase to above 600°C for an irradiation temperature <300°C and to about 200°C for an irradiation temperature of 400°C.

Therefore, being the maximum water temperature, at 15.5 MPa, limited to about 335°C, the use of W-alloy and TZM as structural material has been studied only for comparison but will not be retained.

DESIGN PROPOSALS AND RATIONALE

During the extensive design activities performed for ITER baffles, limiters and divertor, a “monoblock” type concept has been preferred to a “tiles” type concept. Moreover, thermo-mechanical mock-ups tests have shown a better behavior of the monoblock concept.

Therefore, two monoblock type concepts have been considered, both using W-alloy in monoblock geometry as armor material surrounding a tube able to withstand alone the water pressure. A swirl is included in order to enhance the maximum acceptable critical heat flux.

The first concept uses a martensitic steel tube while the second concept uses either a W-alloy or a TZM tube. A thickness of 6 mm have been retained as sacrificial layer for erosion allowance. Monoblock castellation has been extensively applied in order to minimize the thermal stresses. In particular, for the first concept, the initial design foresees W-alloy castellation in the sacrificial layer (the monoblock is therefore continuous along the tube).

On the other hand, the improved design assumes castellation of the whole tube (leading to independent separated monoblocks). Figs. 1 and 2 show the 4 concepts investigated in the analyses : the two first ones (see Fig. 1) consider a steel tube surrounded by monoblocks. In the case of the called "first solution", only the front part of the monoblock is castellated. In the case of the "Improved solution", the whole monoblock is castellated (in the vertical direction). Fig. 2 shows the concepts selected in the case where the tube and the monoblocks are in W . Only the so called "Retained solution" gives interesting results. The W sacrificial layer thickness is in both cases 5.5 mm.

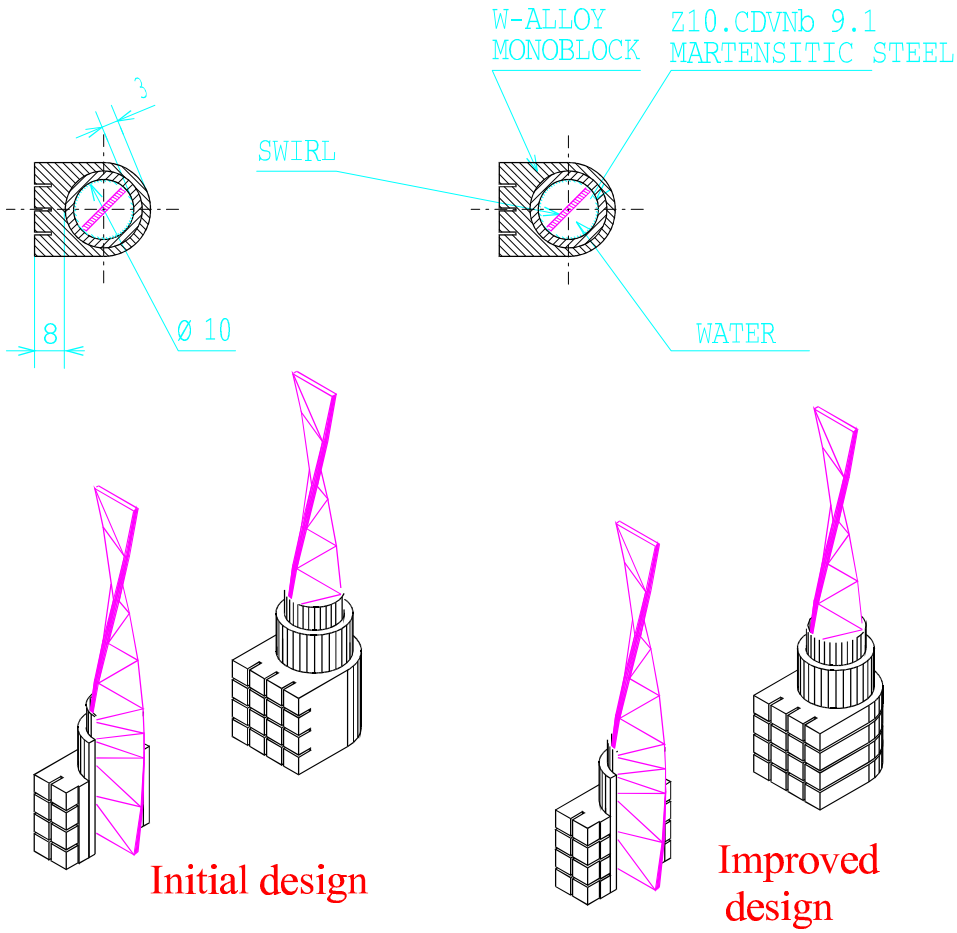

Figure 1 : Water-cooled divertor concept : monoblock with steel tube

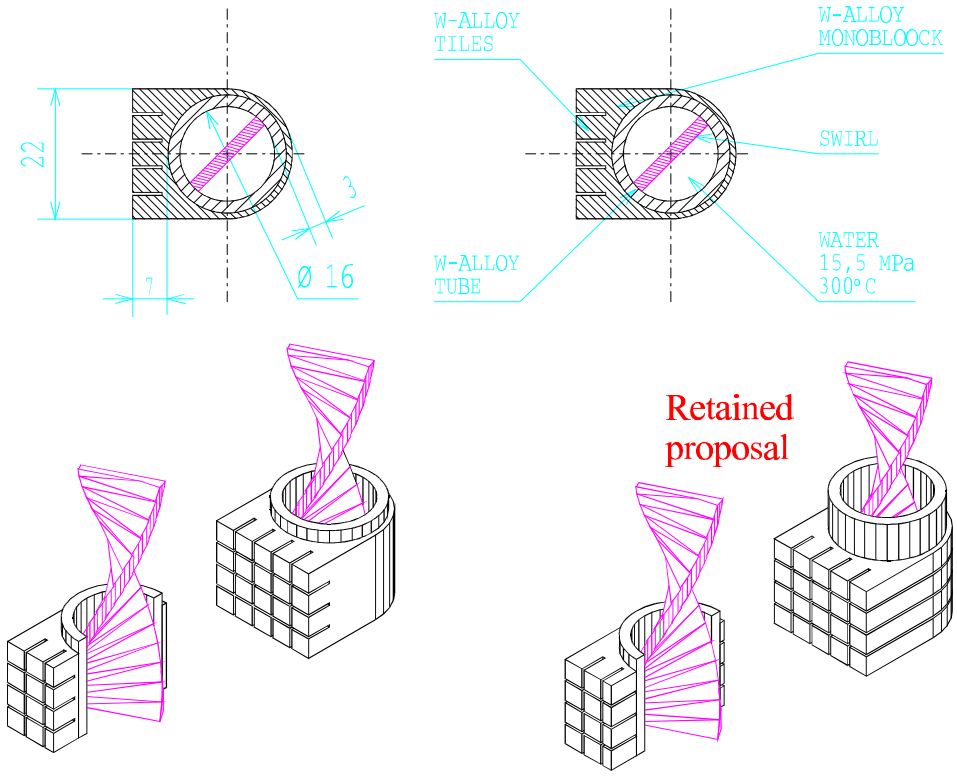

Figure 2 : Water-cooled divertor concept : monoblock with W-alloy or TZM tube

MAIN RESULTS

Analyses have been performed using the CEA finite element code CASTEM 2000, extended with the High Flux Components procedures developed by CEA/DRFC/ Cadarache. Correlation used for Critical Heat Flux is Tong75 (increased by a factor 1.67 due to the swirl). The water coolant main parameters are: inlet temperatures of 150°C, 275°C, 300°C depending on the case, a pressure of 15.5 MPa and a velocity of 5 m/s. Table 1 gives the results for the case with steel tube. It can be seen that, for the "First Solution" using W-alloy, the acceptable incident flux is limited to 3 MW/m² if the coolant is at high temperature, but can be increased to 12 MW/m² by reducing the water inlet temperature to 150°C. By comparison, considering TZM instead of W-alloy in the same conditions lead to an acceptable incident flux of 15 MW/m². The last line of table 1 indicates the acceptable results obtained with the "Improved Solution" with an incident flux of 7 MW/m² and an inlet temperature of 300°C. Fig. 3 shows the temperature distribution for this case.

The parametric study has been also performed for the case without steel tube (tube in W-alloy or TZM). Keeping a inlet temperature of 300°C, the maximum acceptable heat flux is 11 MW/m². By reducing this temperature to 150°C, the concept is able to withstand 14 MW/m² with W-alloy and 16 MW/m² with TZM.

For all the cases studied, the limits of the concepts are always due to thermo-mechanical reasons. In particular, for the concept with steel tube, the high difference between coefficients of thermal expansion for W-alloy and steel is the main limiting factor.

The presence, in between, of a ductile compliant layer could significantly reduce the level of stress. The W sacrificial layer thickness plays two roles : from the thermal point of view, the thickness limits the acceptable flux for selected cooling parameters due to the maximum allowable temperature in the material.

From mechanical point of view, it can be expected that the increase of the temperature due to an increase of the layer thickness will increase the level of stress. Problem of Critical Heat is manageable up to high fluxes (>15 MW/m²). Maximum allowable temperatures of the materials (2000°C for W-alloy and 550°C for steel) are reached for an incident flux of about 16 MW/m².

OPEN ISSUES

Open issues are mainly related to materials and joints. The use of W-alloys (or Mo-alloys) as structural material at relatively low temperature (~300°C) is not acceptable because of their low ductility. The results shown in table 1 for these cases are reported only for comparison with the cases with steel tube. Neutron irradiation even worsen the situation. Improvement of present-day W-alloys and Mo-alloys (e.g., grain size, alloying elements) are required if the advantage of using these materials (acceptability of a larger surface heat flux) has to be exploited. For the use of W-alloys as armor material, a more limited although still significant development is required in order to avoid the problem of W-alloy embrittlement under irradiation. It is not clear if in FPP-divertor temperature below 400°C are allowed (as they are in case of a low-fluence ITER-like machine). Moreover, an appropriate joint technique between martensitic steel and W-alloys have to be developed.

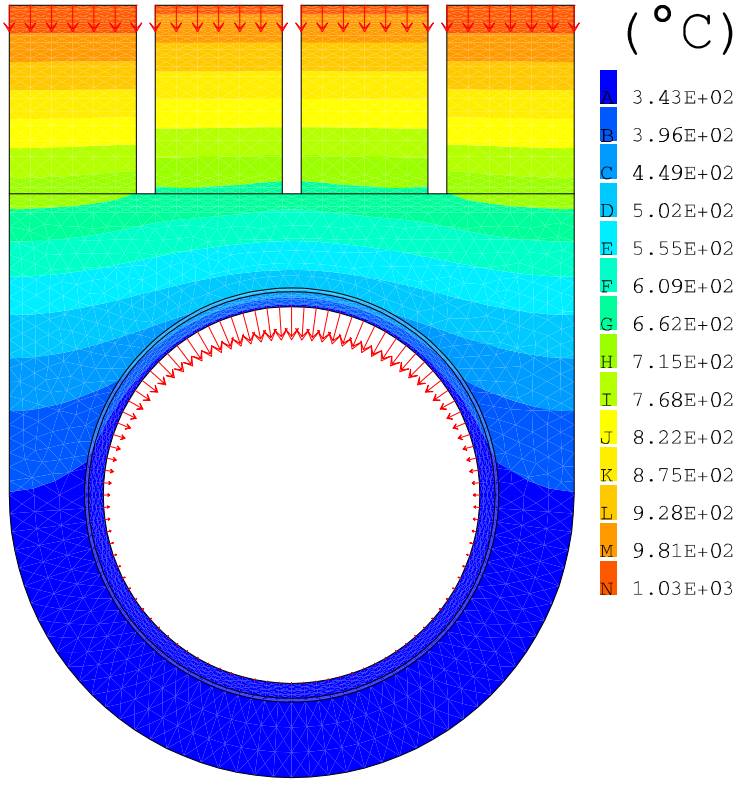

Figure 3 : Temperature distribution for the improved solution of the concept with steel tube for the case of an incident flux of 7 MW/m² and a water inlet temperature of 300°C

Table 1 : Main results for the case with steel tube (without compliant layer)

Geometry	Inc. Flux (MW/m^2)	Water T inl/outl	Tmax (°C) steel	Tmax (°C) W-alloy	DNBR	margin against 3Sm (MPa) monobl	margin against 3Sm (MPa) tube W	margin against 3Sm (MPa) tube steel
First Solution	3	265/273	345	615	8.5	437	402	2
Φ 10 mm	5	150/165	284	725	14	408	509	256
th steel 0.35 mm	10	150/181	407	1334	6.7	158	166	120
th W 8 mm	12	150/187	456	1588	5.4	57	40	49
idem with **TZM**	13	150/190	479	1702	5.0	444	614	98
(instead of Wal)	15	150/195	527	2004	4.2	340	520	31
Improved Solution	7	300/315	494	1061	2.2	263	-	46

CONCLUSIONS

The preliminary assessment has shown that a credible water-cooled design concept exists for use in FPP HHFC (and in particular for the divertor). The concept is based on the use of W-alloy monoblocks surrounding a martensitic steel tube. The water conditions are compatible with that of the WCLL coolant, which means that the power deposited in the divertor region can be used for power conversion. W-alloy castellated monoblock with tube (only hard joint has been evaluated) has the potential for satisfying reasonable FPR divertor operating conditions, provided behaviour under irradiation be improved (need of decreasing DBTT). Tube in martensitic steel, case with lower R&D needs, would allow up to about 7 MW/m² with an inlet temperature of 300°C.

The use of TZM could slightly improve the performances. Tube in W-alloy, case with higher R&D needs, would allow up to about 11 MW/m² at Tinlet = 310°C and to 15 MW/m² at Tinlet = 150°C. Again, the use of TZM could slightly improve the performances, and also solve an eventual problem of low DBTT which could occur for W-alloys (as structural material). These limits are thermo-mechanical limits. No problem related to Critical Heat Flux has been found. Then, improved performances can be expected if soft joints (ductile layer between tube and monoblocks) can be used. W-alloy behaviour under irradiation, fabrication (especially for tubes) and joints are the main R&D issues. Other potential issues are those related to n-induced activation (e.g., short & long term activation, afterheat). TZM is worst from this point of view.

PUBLICATIONS

[1] L. Giancarli, J.F. Salavy, Performance and feasibility of Water-cooled High Heat Flux components, CEA report DRN/DMT SERMA/LCA/RT/99-2684/A, December 1999.

TASK LEADER

Luciano GIANCARLI

DRN/DMT
CEA Saclay
91191 Gif-sur-Yvette Cedex

Tél. : 33 1 69 08 21 37
Fax : 33 1 69 08 99 35

E-mail : luciano.giancarli@cea.fr

PPA 1.4.1

Task Title : HIGH HEAT FLUX COMPONENTS
Liquid metal cooled High Heat Flux Components

INTRODUCTION

Liquid metal cooling has the potential for high power density, low pressure and high coolant temperatures suitable for high efficiency power conversion systems. One possibility is to remove the heat by forced convection, employing relatively high velocity and insulating coatings on all channel walls, or flow channel inserts. The potential of high heat flux components with liquid metal convection is assessed with respect to heat flux capability, operational temperature/pressure limits, structural material requirements, availability, and the impact on the overall reactor system. The work was performed in the framework of the subtask PPA 1.4.1 which concerned the assessment of forced convection cooled liquid metal divertors.

1999 ACTIVITIES

The assessment aimed at evaluating the maximum allowable peak heat flux. It has been assumed that a uniform surface heat flux is deposited on a length of 50 cm of the divertor armor. A case with a peaked distribution of the heat flux was also studied. A fixed volume heat flux per material corresponding to a neutron wall loading of 1.2 MW/m^2 was also included.

RATIONALE OF THE MATERIALS PROPOSAL

Two liquid metals have been selected because of their low reactivity with air and water: the Pb-17Li (melting point 235°C) and SnLi (assumed melting point 330°C).

For structural material, it appears that W-alloys is the best choice as armor material, while the same W-alloy, Mo-alloys (e.g., TZM) and martensitic steel and possibly SiC_f/SiC are the best performing structural materials.

However, only W-alloys have been considered in the present study because better thermo-mechanical performances are expected.

As far as electrical insulators are concerned, SiC_f/SiC has been selected taking into account the assumptions concerning characteristics and design criteria defined in the TAURO studies, assuming for instance a maximum operating temperature of 1300°C (which is the expected out-of-pile value for the new type-S SiC fibers under development within EU).

PROPOSED DESIGN AND RATIONALE

Several concepts with different advantages and drawbacks have been evaluated : i) round W-alloy tubes surrounded by W-alloy monoblock; ii) square W-alloy tube with castellated plasma-facing wall (see Fig. 1); iii) square W-alloy tube with porous plasma-facing wall.

In order to avoid unacceptable MHD pressure-drops, in each tube a SiC_f/SiC flow channel inserts acts as electrical insulator.

Geometrical data have been studied in a parametric analysis by varying the various dimensions (diameters, thickness, etc.). The results presented have been obtained considering the geometries which take into account the best dimensions for each concept.

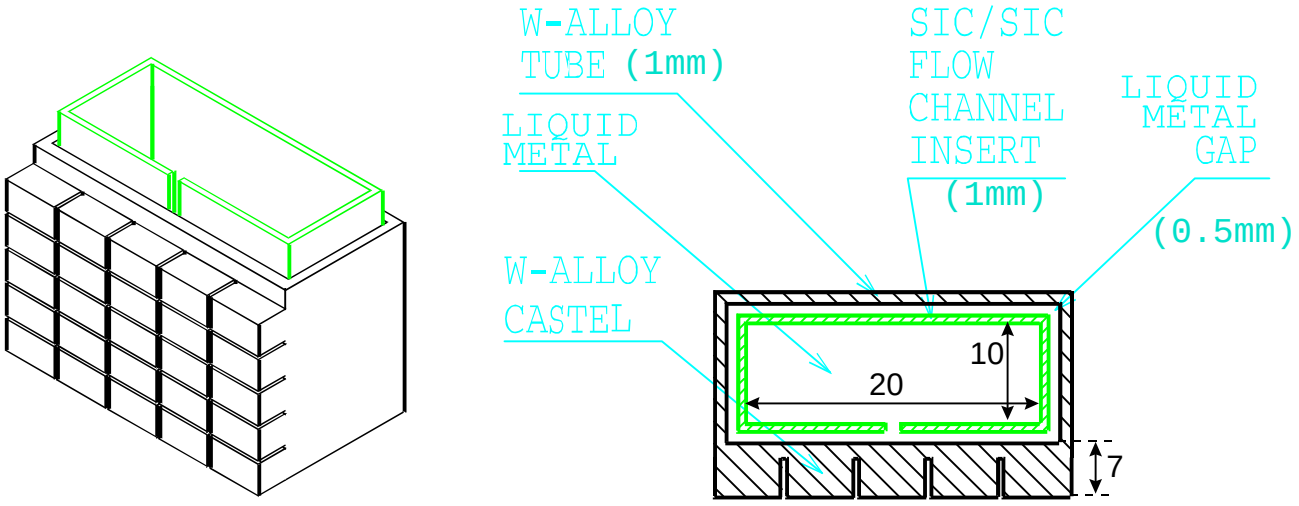

Figure 1 : W1%La_2O_3 castellated square tube, SiC_f / SiC flow channel insert

MAIN RESULTS

For all concepts, thermo-mechanical analyses have been performed using the CEA finite element code CASTEM 2000. In all cases, the assumed liquid metal pressure corresponds to a hydrostatic pressure of 0.3 MPa. Only conduction has been assumed between LM and walls. Thermo-mechanical calculations were performed in transient where the time represents the velocity of the liquid metal. The analyses have been performed with the objective to maximise the acceptable surface heat flux. For a given heat flux, the minimum acceptable LM velocity has been retained.

A first set of thermal calculations was performed using the assumption that mixing occurs in the LM coolant (turbulences due to the high velocity in a small channel) and as a consequence an increase by a factor 10 was applied on the thermal conductivity (λ) of the coolant (the only way to simulate convective mixing by a thermal conduction model). This assumption was later invalidated by MHD experts. However, analyses performed with this assumption and the results have been used to compare the potential of each concept before launching more detailed analyses.

Table 1 summarised the results for the 3 studied concepts with the assumption of the increased thermal conductivity. It can be seen from this table that the small advantage in terms of acceptable flux due to the use of the porous FW design cannot justify the development of such an advanced concept.

The results between the round and the square concept are quite similar. Taking into account the fact that the flat velocity profile used in the calculation is too optimistic in the case of the round tube concept, it has been decided to keep only the square tube design for further analyses.

The more interesting results are summarised in Table 2. The "square tube" design being the best performing one, only results concerning this concept are given. Several cases with different inlet LM temperatures are shown in Table 2 in order to investigate the sensitivity to this parameter. Only pure conduction was assumed through the LM (no mixing allowed). The only cases fulfilling the requirements are those with LM inlet temperature of 500°C. For both Pb-17Li and SnLi, the resulting maximum acceptable surface heat flux is 5 MW/m^2, obtained with a similar LM velocity of about 2 m/s.

Table 1 : Main results for the cases with increased conductivity

Coolant **(λ x 10)**	Velocity (m/s)	Inc. Flux (MW/m^2)	Coolant T inl/outl	Tmax (°C)			Margin against 3Sm (MPa)
				W-all	SiC/SiC	flow. lm	
Monoblock + Round Tube							
Pb-17Li	0.5	6	275/460	1858	1185	767	70
Pb-17Li	1.7	8	275/345	2118*	1184	626	9
SnLi	2.5	8	360/410	2113*	1131	584	8
Square Tube							
SnLi	1.7	8	360/483	1714	1044	604	5
	1	7	360/556	1654	1062	670	53
Porous FW							
SnLi	1.7	8	360/475	1258	1040		3
	2.5	9	360/421	1114	899		42

** max. temperature in the front part could be reduced by a decrease of the thickness of the protective layer*

Table 2 : Main results for the retained concept (final results)

Square Tube design - Structures/armor W1%La_2O_3 - SiC/SiC Flow channel insert							
Liquid Metal coolant	Heat Flux (MW/m^2)	Minimum Vel. (m/s)	Coolant T in/out (°C)	T min / T max (°C)			Margin to $3S_m$ (MPa)
				W-alloy	SiC/SiC	coolant	
Pb-17Li	6	2.5	360/447	392/1757	377/1244	363/983	31
SnLi	6	1.7	360/497	395/1774	380/1261	374/998	21
SnLi	*5*	*1.7*	*500/617*	*532/1688*	*518/1262*	*512/1042*	*37*
Pb-17Li	*5*	*2.0*	*500/594*	*531/1708*	*517/1279*	*505/1060*	*29*
Pb-17Li (peak)	*8*	*(1.7)*	*fixed 500*	*505/1565*	*500/1017*	*fixed 500*	*> 0*

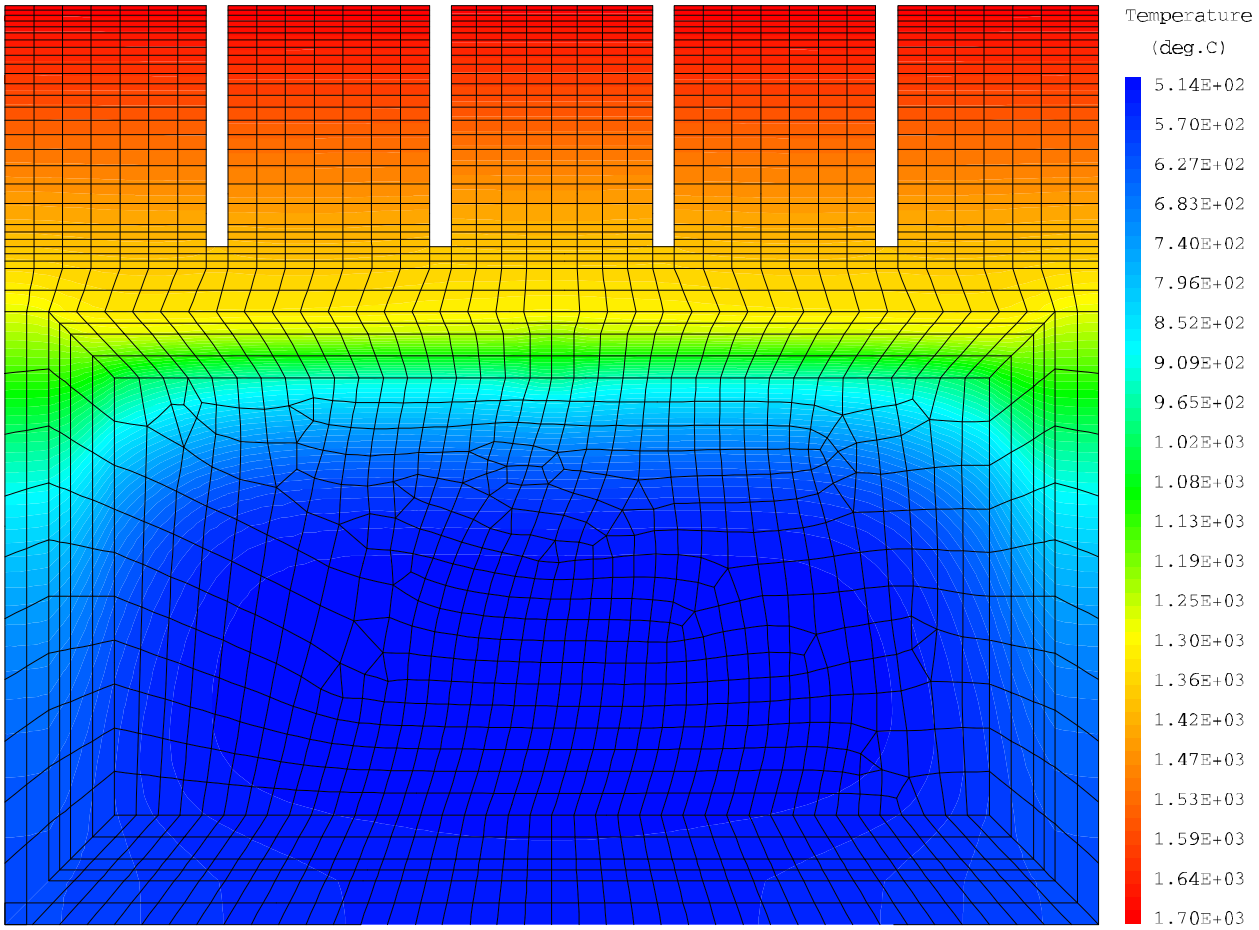

Figure 2 : Temperature distribution in the square tube concept for the case 5 MW/m^2 and Pb-17Li velocity 2 m/s

Figs 2 and 3 give respectively temperature distribution and evolution of the margin against 3Sm as a function of the coolant velocity for the incident flux of 5 MW/m^2 and a Pb-17Li velocity of 2 m/s.

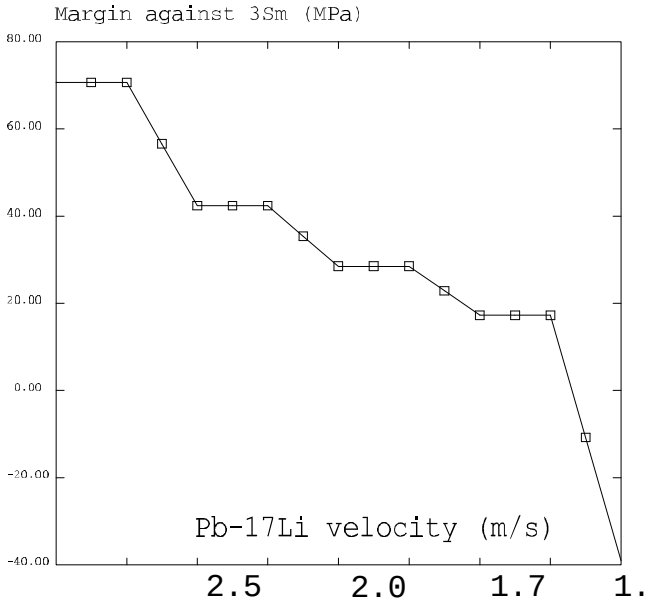

Figure 3 : Evolution of the margin against 3Sm as a function of the Pb-17Li velocity in the square tube concept for an incident flux of 5 MW/m^2

Stresses in the 1 mm-thick SiC_f/SiC flow channel inserts (the possibility of the smaller thickness has not been evaluated) are relatively high but are still considered acceptable in all cases shown in Table 2.

The last case in Table 2 corresponds to the calculation performed at a fixed coolant inlet temperature, which simulates the conditions of a peaked heat flux.

It can be observed that the acceptable surface heat flux is somehow increased (up to 8 MW/m^2) but it does allow for relatively low peaking factors (less than 50%).

OPEN ISSUES

Open issues are mainly related to material characteristics and behavior. Besides the items concerning the materials behavior under irradiation, in particular the low temperature embrittlement of W-alloys under irradiation, major issues are high temperature compatibility between liquid metals and both W-alloys (interface T up to ~1350°C in the static LM gap) and SiC_f/SiC (interface T just below 1300°C in the static LM gap) and front wall erosion from the plasma.

Appropriate R&D has therefore to be launched. Other required R&D for the presently reference concept should address W-alloys joints, W-alloy castellated square tube manufacturing and MHD effects.

CONCLUSIONS

Three different concepts based on LM forced convection cooling were discussed in this report.

They feature similar maximum temperatures of the structural material (preferably W-alloy), low operating pressures and the use of electrically insulating material for the transport of the liquid metal. The most promising design, the square tube concept, allows to remove heat loads of about 5 MW/m^2.

Main open issues are: MHD effects, manufacturing questions for W-alloys, W-alloy under irradiation, the compatibility of the LM with the structural and the insulator material, the high secondary stresses due to large temperature differences, and the low temperature embrittlement of W-alloys under irradiation.

PUBLICATIONS

[1] L. Giancarli, J.F. Salavy, Assessment of forced convection cooled liquid metal divertors, CEA report DRN/DMT SERMA/LCA/RT/99-2683/A, December 1999.

TASK LEADER

Luciano GIANCARLI

DRN/DMT
CEA Saclay
91191 Gif-sur-Yvette Cedex

Tél. : 33 1 69 08 21 37
Fax : 33 1 69 08 99 35

E-mail : luciano.giancarli@cea.fr

PPA 2.1.1

Task Title : FIRST WALL PROTECTION
First Wall influence on blanket performance

INTRODUCTION

In previous blanket studies the impact of the first wall (FW) on the blanket performance was found significant. The objective of this activity was, therefore, to determine the impact of the material composition of the FW onto the blanket performance in terms of tritium (T) permeation, inventory, TBR and power deposition. Various plasma facing materials were compared for their acceptability in a power reactor with focus on T permeation and inventory. Several armor materials compatible with the power plant specifications and the blanket feasibility were selected.

A suitable material for first wall protection should respond at best to the following criteria. Low T permeation and inventory in the FW call for a material with:

- low diffusivity D and low Sieverts'constant K_s to minimize the permeability $D \times K_s$
- high sticking coefficient or recombination coefficient on the plasma side,
- low sticking coefficient on the coolant side,
- low concentration of ion and neutron induced traps,
- low trapping energy.

1999 ACTIVITIES

A literature review was performed to confront several materials with the requirements above. In Figures 1 and 2 the Arrhenius plots for D and K_s are shown. For the metals, the lowest D and K_s are found for Be and W whereas V and its alloys and Ta show the highest values. TZM, a Mo alloy, has a low D but a high K_s. Concerning the non-metals, C and SiC have a low D but a high K_s.

The macroscopic values for D and K_s in these materials are controlled by the amount of porosity. The microscopic K_s for C and SiC is determined by trapping in lattice defects which increase with irradiation.

The T permeation through metals is quite sensitive to surface contamination on the plasma facing side following the relation :

$$J_1 = \frac{D}{L}\sqrt{\frac{I}{2K_r}}\left[\frac{at}{m^2 s}\right]$$

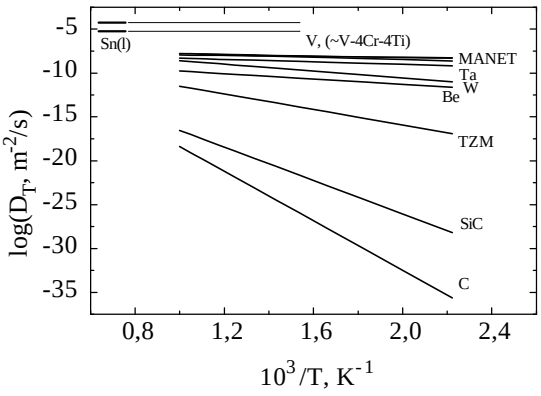

Figure 1 : Diffusivity of tritium in various materials

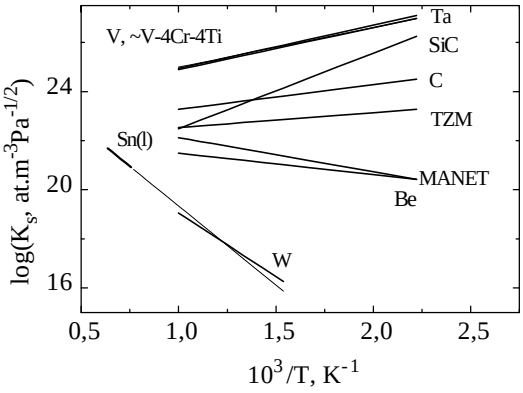

Figure 2 : Sieverts' constant for tritium in various materials

where J_1 is the permeation flux, D the diffusivity, L the metal thickness, I the impinging ion flux and K_r the recombination coefficient.

The recombination coefficient can be expressed as a function of the sticking coefficient :

$$s = s_0 \exp\left\{\frac{-2E_c}{kT}\right\}$$

and the Sieverts' constant $K_s = K_{s0}\exp(-Q_s/kT)$ as follows:

$$K_r = \frac{s\,m}{K_s^2}\left[\frac{m^4}{s}\right]$$

where $m = 1/\sqrt{2\pi m\, kT}$.

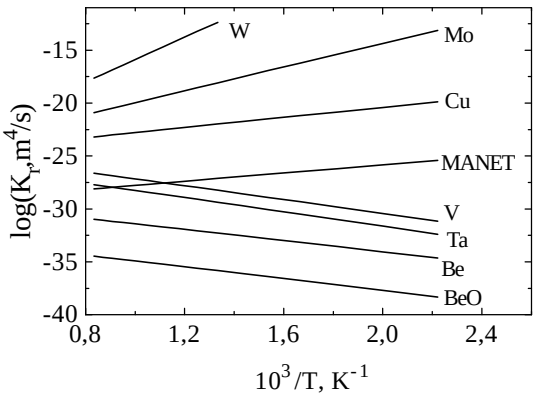

Figure 3 : Recombination coefficient for several materials

Here again, W would be the best material choice compared to uncoated MANET steel, followed by Mo and Cu, whereas Be and BeO are significantly worse at typical FW temperature (500°C).

With the material properties the ion driven permeation flux from the plasma into the coolant was calculated assuming a FW thickness of L = 3 mm and an incident tritium ion flux $I = 1.5\times10^{20}$ ions.m^{-2} s^{-1}.

As there are still significant uncertainties concerning the surface conditions, this was done for two distinct cases.

- « Bare » plasma facing surface. Figure 4 shows an Arrhenius plot for the expected ion driven permeation for a surface state that was experimentally shown to be achievable (different sticking coefficients depending on material).

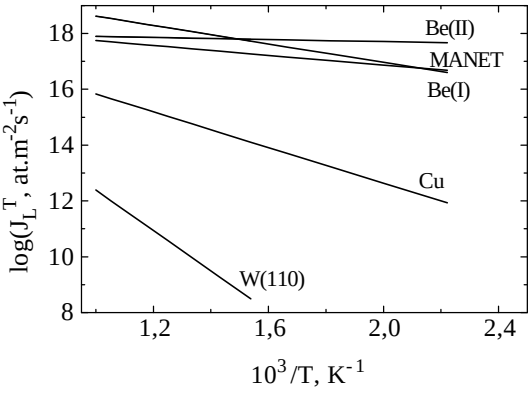

Figure 4 : Ion driven tritium permeation for different materials with realistic sticking coefficients

- Perfectly clean plasma facing surface. Figure 5 shows an Arrhenius plot for the expected ion driven permeation for an ideally clean surface state, i.e. a sticking factor s = 1.

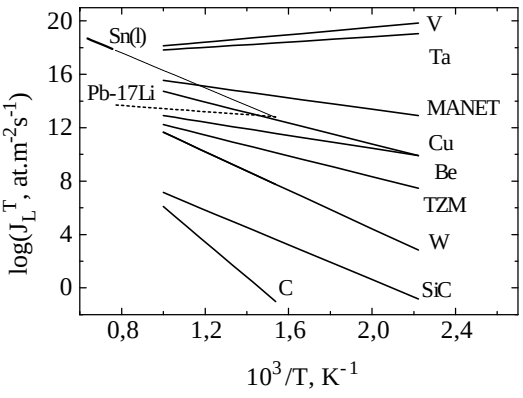

Figure 5 : Ion driven tritium permeation for different materials with ideally clean surface

CONCLUSIONS

From Figures 4 and 5 the following conclusions can be drawn :

1. For both clean and « bare » plasma facing surfaces, the T permeation through W is the lowest.

2. The permeation through Be for bare conditions may be higher than through MANET at T < 650 K owing to the low sticking coefficient for Be.

3. The "apparent" permeation through SiC and C is lower than through metals.

4. SiC and C retain T until the surface layer becomes amorphous. The permeation through SiC and C cannot be modeled correctly with a recombination factor and is strongly dependent on the porosity of the ceramic.

5. T permeation is high for V and Ta, but small for W and TZM.

6. T permeation through MANET and Be with a "bare" surface is high but low if sputter-cleaned to s = 1.

7. T permeation through SiC and C is probably low, but strongly dependent on porosity (new model required).

8. The time to reach steady-state is long for materials with low diffusivity and high trapping, e.g. W, Be, C, SiC.

9. The T inventory is dominated by T in traps (neutron and ion induced), in porosities and in chemical compounds (if applicable). The inventory in solution is comparatively small.

10. W has the lowest T permeation and inventory, best thermal properties and low erosion rates. But its application as FW armor induces a sensible reduction in TBR and causes problems with fabrication, joining and afterheat.

11. V alloys and Ta show the highest permeation (no problem in self-cooled Li concepts) but also very high inventory. From a T point of view, they are the least suitable.

12. C and SiC have low permeation but high inventory due to the required porosity (mechanical properties). The formation of chemical compounds should be reduced.

13. RAFM steel without armor material may be acceptable if the plasma facing surface is clean ant the coolant side is oxidized. Be armor would decrease the permeation but increase the inventory. This may cause problems with respect to lifetime (high erosion rates expected), fabrication, T accounting and possibly TBR.

These results on the T related behavior will still need to be completed by neutronics calculations to better estimate the influence on TBR and power deposition. Further analysis seems also required concerning the lifetime of the FW material due to special plasma-surface interaction effects (cf. Executive Summary for PPA 1.1).

PUBLICATIONS

[1] O. V. Ogorodnikova, M. A. Fütterer, Impact of the first wall on tritium permeation of power blankets, CEA report DRN/DMT SERMA/LCA/RT/99-2712/A, December 1999.

TASK LEADER

Michael A. FÜTTERER

DRN/DMT/SERMA/LCA
CEA Saclay
91191 Gif-sur-Yvette Cedex

Tél. : 33 1 69 08 36 36
Fax : 33 1 69 08 99 35

E-mail : michael.futterer@cea.fr

UT-SM&C-VVI

Task Title : DESIGN AND ANALYSIS OF VACUUM VESSEL AND INTERNALS

INTRODUCTION

The task UT-SM&C-VVI is a contribution to the European Fusion Underlying Technology Program. This task is intended to maintain/develop competence and analysis tools in the field of the design of tokamak vacuum-vessel and internals (divertor, limiters, baffle, first wall, shielding blanket and breeding blanket).

1999 ACTIVITIES

The activities in 1999 covered comparative analysis work on plasma facing materials on the one hand and more specific conceptual design work on the other.

PLASMA-FACING MATERIALS

Plasma-facing materials for in-vessel components of fusion reactors should satisfy the following criteria: good thermal properties (high melting point and thermal conductivity). good mechanical properties (low crack growth rate under cyclic stresses), low erosion, low hydrogen isotope permeation and inventory, and low activation. Low-Z materials (C and Be) ensure low impurity radiation in the plasma but exhibit high erosion rates. On the other hand, high-Z materials (Ta, W) have a lower erosion rate but can produce high impurity radiation in the plasma even at low concentration.

For example, for a DT plasma at 10 keV, the maximum allowable impurity fractions are: Be $\approx 10^{-2}$; V, Ti, Fe $\approx 10^{-3}$ and W, Ta $\approx 10^{-5}$. Some recent calculations have shown that the net-erosion rate (sputtering minus re-deposition) of Be would range between 1 - 10 nm/s, while lower erosion rates were evaluated for W, i.e. 0.01 - 0.1 nm/s. Endothermic metals such as Be, W, Cu, and martensitic 7-10% Cr steels (typical examples with an acceptable data base are MANET and F82H) were compared to exothermic metals such as TZM (a Mo alloy), V, Ti and Ta in terms of hydrogen isotope permeation and inventory. Non-metals such as CFC (carbon fiber composites) or β-SiC and liquid metals such as Pb-17Li or Sn were also investigated.

The increase of both diffusion coefficient D and Sieverts' constant K_s results in the increase of permeation. Consequently, a metal should have low diffusivity and low solubility to reduce the tritium permeation. Data for hydrogen isotope diffusivity and solubility are listed in Table 1. The lowest diffusivity for metals is found in Be and the lowest solubility in W, while V and its alloys show the highest D and K_s.

Thus, the highest permeation flux for ideally clean surfaces must be expected for V and the lowest for W at a typical First Wall operating temperature of approx. 500°C (Fig. 1):

$$J_L^V > J_L^{Ti} > J_L^{Ta} > J_L^{MANET} > J_L^{Cu} > J_L^{Be} > J_L^{TZM} > J_L^W$$

The conclusions of the work show that a low tritium permeation and inventory can be achieved by a material with:

- low diffusivity D,
- low solubility K_s,
- high sticking coefficient s^0 (or recombination coefficient) on the plasma-facing side,
- low sticking coefficient s^L on the coolant side,
- low concentration of ion and neutron induced traps,
- low trapping energy.

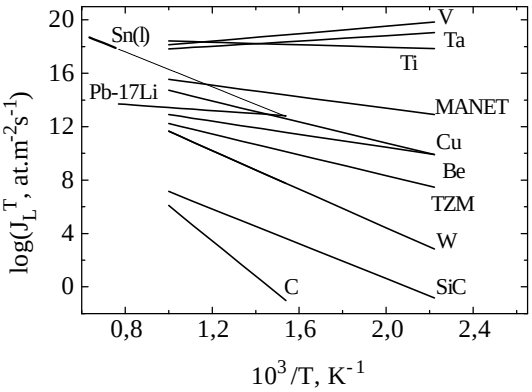

Figure 1 : Ion-driven tritium permeation vs. temperature for perfectly clean plasma-facing surface, extrapolated value for Sn(l) is shown as dashed line

Using these criteria, we conclude that from a tritium permeation and inventory point of view:

1. W is the most suitable metal.

2. Cu also exhibits low permeation and inventory compared to other metals.

3. The tritium permeation is small for TZM but its inventory is high.

4. The tritium permeation through MANET and Be with a bare (slightly contaminated) front surface is high, but with a sputter-cleaned front surface becomes rather low. For a bare surface, the tritium permeation through Be may be higher than through MANET owing to the low sticking coefficient for Be.

5. The most unsuitable metals are V, Ti and Ta because of both high tritium inventory and permeation. However, the tritium permeation and inventory in the exothermic metals can be considerably reduced by contamination (e.g. by oxidation) on the back side. Conversely, the reduction of the sticking coefficient on the back side has less influence on the permeation and inventory for endothermic metals where the sticking coefficient on the front side has a dominating influence.

6. The tritium inventory is dominated by tritium in traps (neutron and ion induced), in porosity and in chemical compounds (if applicable). The inventory in solution is comparatively small.

7. The tritium concentration in Be can reach very high values and can be comparable to the concentration in Ta, Ti and V or even higher.

8. The 'apparent' permeation through SiC and C is lower than through metals but the inventory is high. SiC and C retain tritium until the surface layer becomes amorphous. At some ratio T/C (or T/SiC), no tritium is retained. The permeation through SiC and C cannot be modelled correctly with a recombination factor and is strongly dependent on the porosity of the materials.

9. Similarly to SiC and C, the tritium permeation and inventory in Be are also dependent on the porosity due to fabrication and irradiation effects.

Table 1: Data of diffusivity and solubility of hydrogen isotopes for several fusion reactor materials

Materials	Diffusivity		Solubility	
	$D_0(m^2/s)$	E_m (eV)	K_{s0} (at./m$^3\sqrt{Pa}$) $\times 10^{23}$	Q_s (eV)
α-Fe	3.87×10^{-8}	0.045	6.14	0.27
D_2/F82H	1.07×10^{-7}	0.144	4.54	0.278
D_2/MANET	1.01×10^{-7}	0.137	3.25	0.276
D_2/99.8%Be	6.7×10^{-9}	0.3	—	—
T_2/Be	—	—	0.23	0.173
H_2/W	4.1×10^{-7}	0.39	17.7	1.03
H_2/Cu	1.1×10^{-6}	0.4	4.1	0.37
H_2/α-V	3.5×10^{-8}	0.05	1.51	-0.34
H_2/α-Ta	4.4×10^{-8}	0.14	1.5	-0.35
H_2/α-Ti	1.45×10^{-6}	0.55	5.2	-0.47
D_2/BeO	1.31×10^{-9}	1.335		
BeO			9.4×10^{-6}	0.8
H_2/TZM	5.5×10^{-5}	0.88	8.5×10^{-3}	-0.12
Sn(l)	1×10^{-4}	0	6.2×10^{2}	1.28
T_2/Pb-17Li(l)	2.33×10^{-8}	0.195	8.433×10^{-3}	0.0135
C (CFC)	9.3×10^{-5}	2.8	1.85×10^{22}	-0.2
β-SiC	9.8×10^{-8}	1.89	2.6×10^{-4}	-0.61

THERMAL-HYDRAULICS MODELS FOR LIQUID METAL COOLED COMPONENTS

In a first analytical analysis, we have tried to establish a preliminary estimation of the temperature field in the Pb-17Li flow. The cooling of the divertor is regarded as the equivalent 2D problem. The main problem of this first approach was that it overestimated the temperature field. This overestimation has two reasons: firstly, the fluid flow is restricted to laminar flow, and, secondly, the temperature profile is not calculated in the entrance length. A 2D or 3D numerical model could be realized in order to design the castellated square tube. Recently, fluid mechanics operators were developed for the CASTEM 2000 code to solve the Navier-Stokes equation in laminar or turbulent incompressible flow associated with the energy equation, thus enabling to solve a fully coupled thermo-hydro-mechanical problem.

The principle could be to solve first the equations of mass, momentum and enthalpy conservation in the fluid and the enthalpy conservation in the solid for a full 3D model (including structural material and coolant) with appropriate boundary conditions to obtain the temperature, velocity and stress fields.

This method could allow a fully 3D coupled calculation including steady state and transient. However, the "fluid" part of the CASTEM 2000 code was not fully developed and documented in 1999.

It was not possible yet, in terms of time and investment, to use it for the dimensioning of forced convection cooled liquid metal divertor concepts (parametric analysis) performed in the framework of the preparation for a power plant conceptual study performed during 1999 (cf. PPA 1 tasks).

A simplified model, used up to now to solve liquid metal cooled problems is described in detail and commented on two representative cases. A 2D section of the concept is used, the liquid metal being included in the meshing.

Thermal calculations are performed in transient where the time represents the velocity of the liquid metal. Only conduction has been assumed between LM and walls thus taking due account of the expected MHD effect.

The velocity profile is flat and the axial conduction is not taken into account.

This first transient thermal calculation yields an evolution of temperature distributions as function of time (in fact the position), each of them can be used in a steady-state 2D thermo-mechanical calculation. Special assumptions have to be taken into account, in particular the specific heat of the non-flowing materials, initial temperature distributions and boundary conditions. The description of the method is given first on the case of the convectively cooled liquid metal divertor, castellated square tube concept, for an inlet Pb-17Li temperature of 500°C and an incident flux of 5 MW/m^2 on 0.5 m length. Fig. 2 shows the temperature distributions at the outlet section for 3 different Pb-17Li velocities, 1.7, 2 and 2.5 m/s.

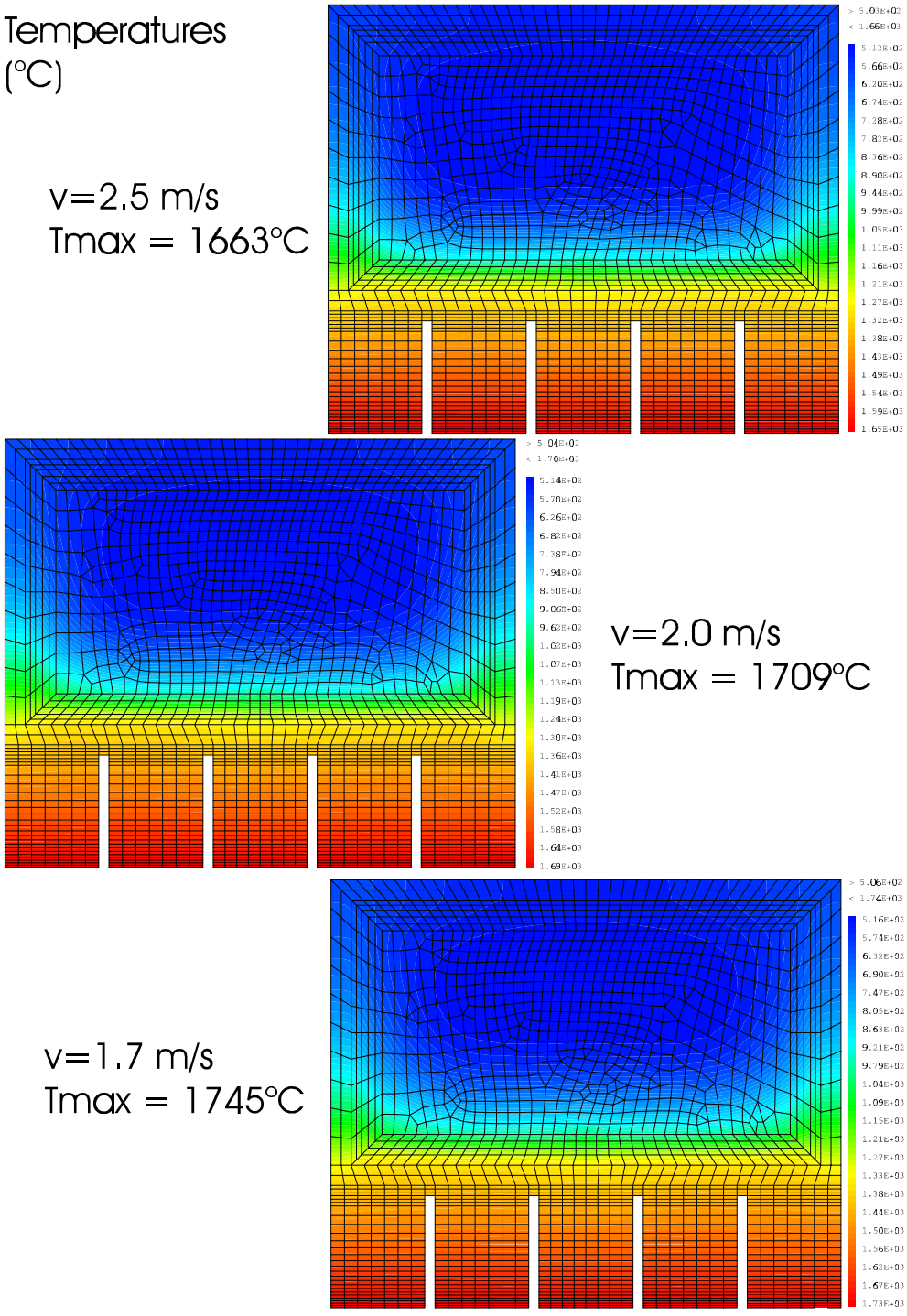

Figure 2 : Temperature distributions for the castellated square tube divertor concept

At this step of the method, thermal results are saved and will be used as input of the thermo-mechanics. For a parametric analysis, the simple thermo-mechanical method is to treat temperature distributions at each transient time as a on in steady-state, and to make a steady state 2D mechanical analysis assuming this thermal load. In this case, it is considered that the whole structure has this thermal distribution, the axial variation is not taken into account.

A 2D generalized plane strain analysis is performed for each temperature distribution (successive mechanical steady states) and the evolution of the margin against the 3 S_m criterion results in the minimum acceptable velocity for the liquid metal. Fig. 3 shows the evolution of the margin against 3 S_m vs. the Pb-17Li velocity in the case of a square tube concept with an incident flux of 5 MW/m^2 and an inlet temperature of 500°C.

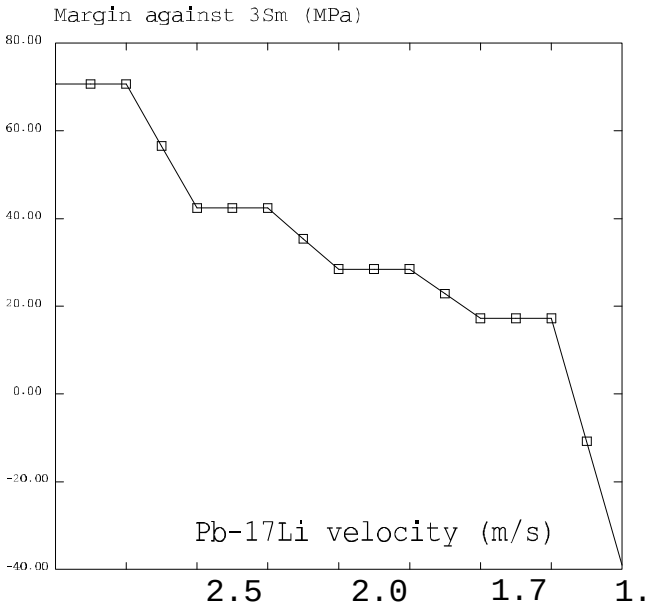

Figure 3 : Evolution of the margin against $3S_m$ vs. the Pb-17Li velocity for the castellated square tube divertor concept

This simplified model has also been used in the case of a multi-directional flow pattern, in the case of the TAURO blanket where the liquid metal cools first the first wall by flowing down in a small annular channel, then flows up in a second half circular channel, then down and up again in the following square channels, the velocity being different in each channel. In this case, the thermal transient calculation is repeated for each channel and it is then necessary to reach a convergence in term of temperature (equivalent to a zero exchange flux) at the interface between adjacent channels. In order to perform the thermo-mechanical calculation, it is then necessary to project these temperature distributions of a full 3D model including all the channels.

The thermal resultant load is finally a 3D steady-state temperature distribution on the whole model, even if it has been obtained by several transient calculations on partial 2D meshes.

CONCLUSIONS

The activities performed within the UT-SM&C-VVI task have covered two important fields of activity, work on plasma facing materials on the one hand and thermal-hydraulics computation methods on the other. Main achievements in 1999 have been the evaluation of criteria for plasma facing components in order to achieve low tritium permeation and inventory, and the various candidate materials have been compared using these criteria. Problems of liquid metal self-cooled components have been analysed in detail. Even if was not possible yet to use the "fluid" part of the CASTEM 2000 code to solve a fully coupled thermo-hydro-mechanical problem, a simplified method has been developed and used for dimensioning several components.

PUBLICATIONS

[1] O. V. Ogorodnikova, M. A. Fütterer, Tritium related aspects of materials for in-vessel components of fusion reactors, CEA report DRN/DMT SERMA/LCA/RT/99-2711/A, December 1999.

[2] M. A. Fütterer, G. Aiello, F. Gabriel, J.-F. Salavy, Thermal-hydraulics models for liquid-metal cooled Vacuum Vessel Internals, CEA report DRN/DMT SERMA/LCA/RT/00-2755/A, February 2000.

TASK LEADER

Luciano GIANCARLI

DRN/DMT/SERMA/LCA
CEA Saclay
91191 Gif-sur-Yvette Cedex

Tél. : 33 1 69 08 21 37
Fax : 33 1 69 08 99 35

E-mail : luciano.giancarli@cea.fr